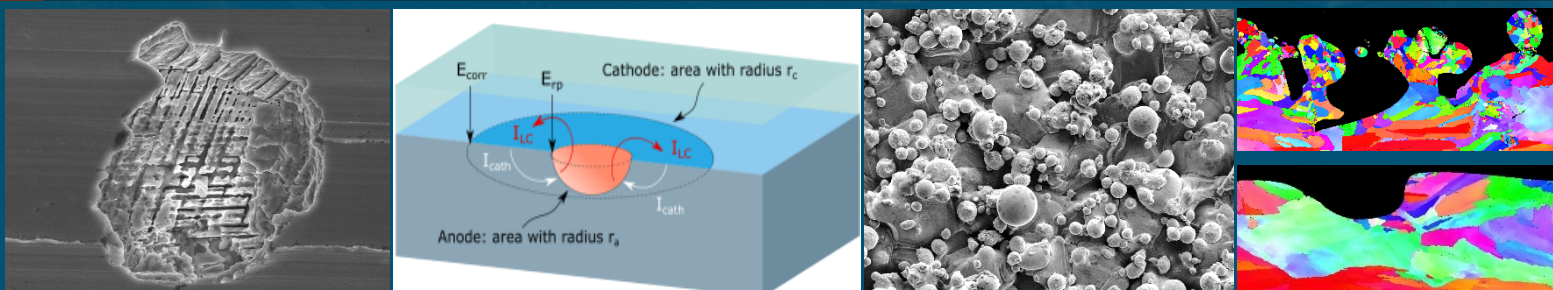


How part surfaces influence corrosion for a laser powder bed fusion 316L stainless steel

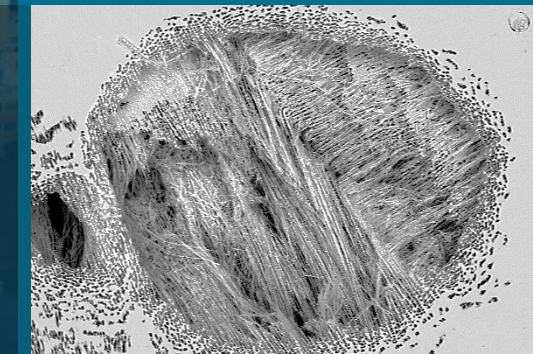


PRESENTED BY

Michael Melia

TMS 2022
February 27–March 3,
2022
Anaheim, California, USA

Contributors: Erin Karasz, Kasandra Escarcega-Herrera, Jay Taylor, Samantha Rosenberg, Paul Kotula, Michael J. Heiden, Jeffrey M. Rodelas



Sandia National Laboratories is a multimission laboratory managed and operated by National Technology and Engineering Solutions of Sandia, LLC, a wholly owned subsidiary of Honeywell International Inc. for the U.S. Department of Energy's National Nuclear Security Administration under contract DE-NA0003525.

Process flow map for metal AM component



Component design/optimization

- Topology optimization
- Improve functionality/product reliability
- Reduced cost/material waste

Material choice/development

- Improved properties
- Reduce constraints

Process

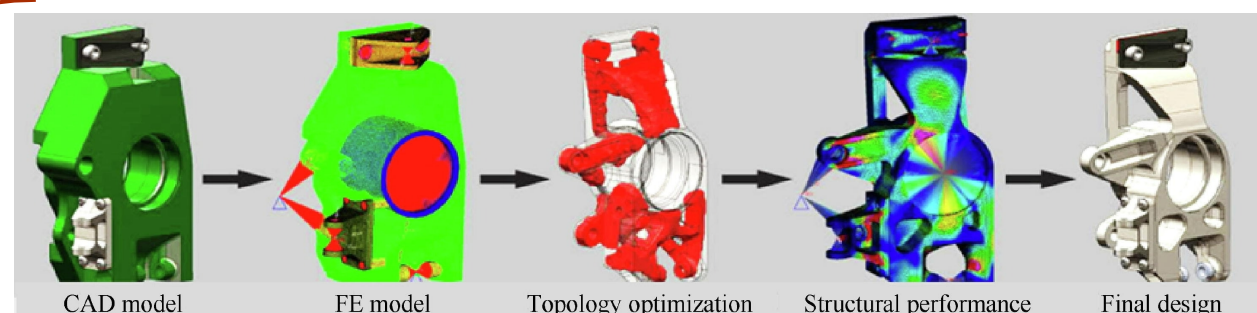
- Select manufacturing technique
- Process optimization
- Print components

Post processing

- Remove components from build plate
- Stress relief
- Machining/surface finishing

Quality assurance

- Specification and standards testing & failure analysis
- Reduced risk



J. Zhu, et al., Chinese Journal of Aeronautics, (2021).

Material Classification

Stainless steel

UNS/Similar product

S15500/15-5PH

S17400/17-4PH

S30403/304L

S31603/316L

Ni-based Superalloy

N06625/Ni alloy 625

Ni-Fe Superalloy

N07718/Ni alloy 718

Co-based Superalloy

R31537/CoCr

High Performance Titanium

R56400/Ti6Al4V

Aluminum Alloy

AlSi10Mg

Process flow map for metal AM component



Component design/optimization

- Topology optimization
- Improve functionality/product reliability
- Reduced cost/material waste

Material choice/development

- Improved properties
- Reduce constraints

Process

- Select manufacturing technique
- Process optimization
- Print components

Post processing

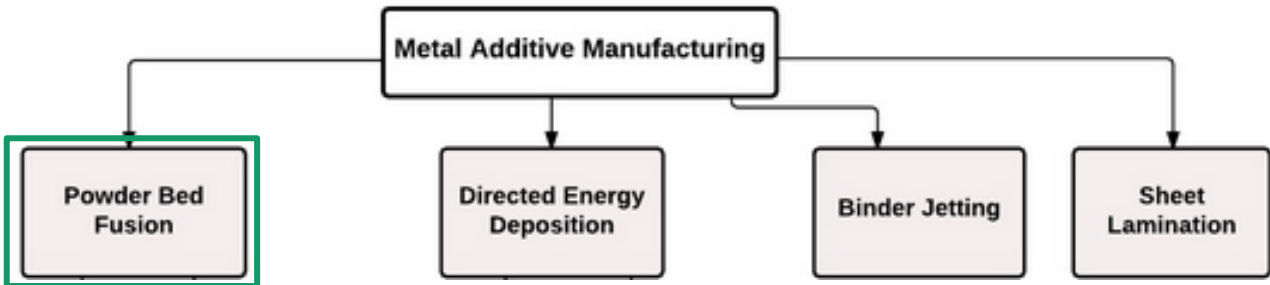
- Remove components from build plate
- Stress relief
- Machining/surface finishing

Quality assurance

- Specification and standards testing & failure analysis
- Reduced risk

Industrial-Grade Metal Additive Manufacturing Machines

- Available for Purchase* -



- Optimize parameters
- Machine upkeep
- Build size/speed
- # of parts per build

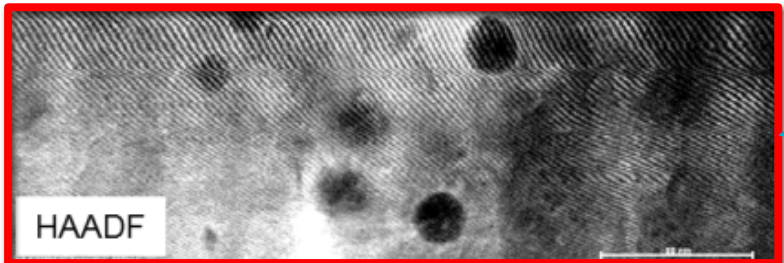
Microstructural features from powder metal AM



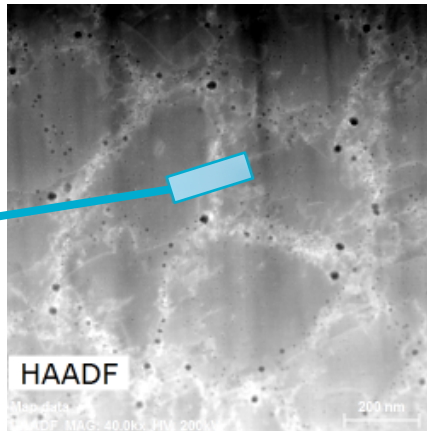
Chemical heterogeneities

Cell walls decorated with oxides

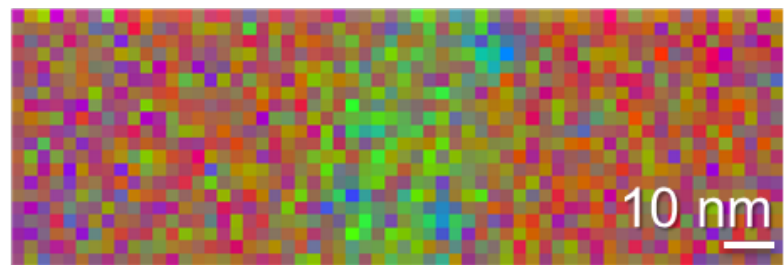
Matrix Cell Boundary Matrix



HAADF



HAADF

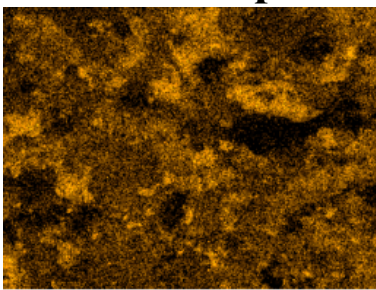


Adapted from Schaller, 2018

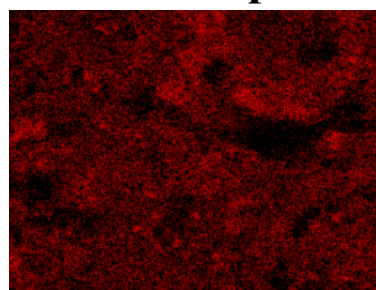
- Increased Fe (+ 9%)
- Increased Si
- Increased Cr (+ 4%)

Recast layer from a part removed with wire EDM

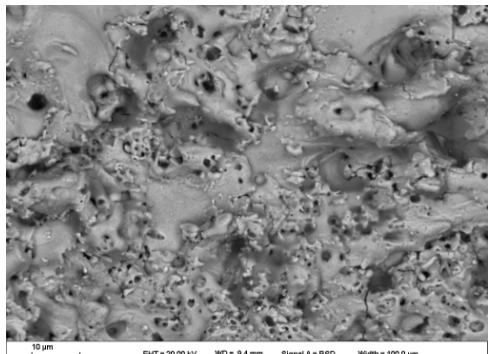
Cu map



Zn map

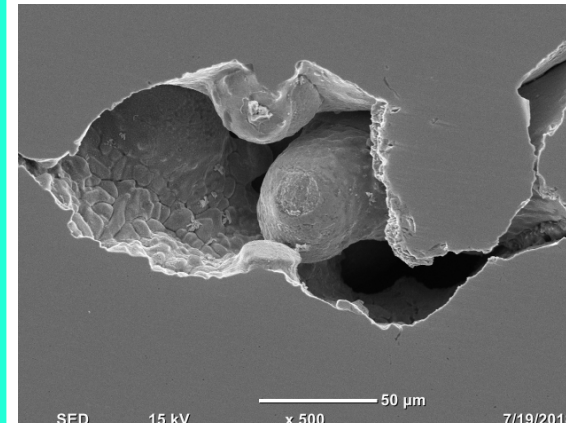


Cu and Zn penetrate 5 to 10 μm deep.

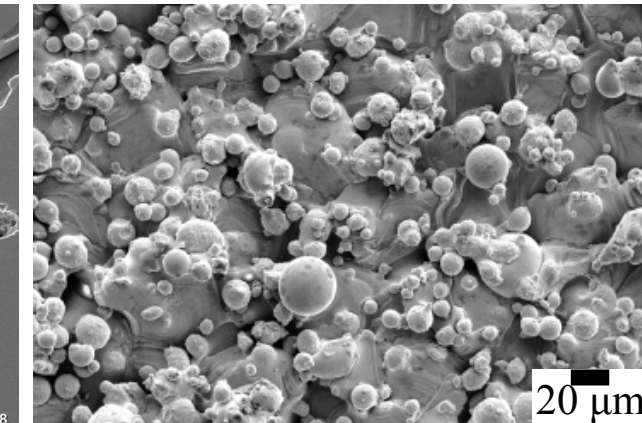


Processing defects

Porosity



Melia, 2019



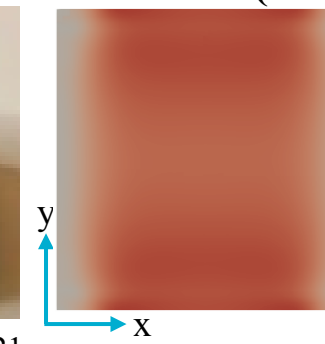
Melia, 2020

Residual stress of 316L cubes

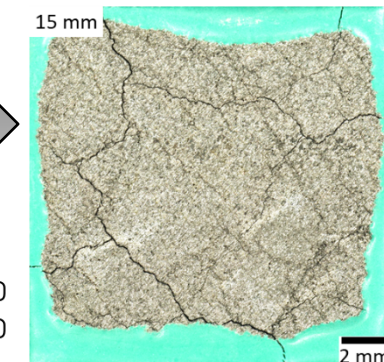
Stress XX (MPa)



Karasz, 2021



200
100
0
-100
-200



Leads to susceptibility to stress corrosion cracking

(UUR)

Process flow map for metal AM component



Component design/optimization

- Topology optimization
- Improve functionality/product reliability
- Reduced cost/material waste

Material choice/development

- Improved properties
- Reduce constraints

Process

- Select manufacturing technique
- Process optimization
- Print components

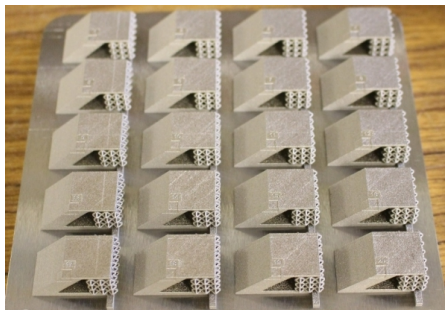
Post processing

- Remove components from build plate
- Stress relief
- Machining/surface finishing

Quality assurance

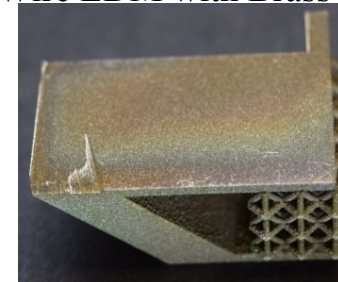
- Specification and standards testing & failure analysis
- Reduced risk

(UUR)

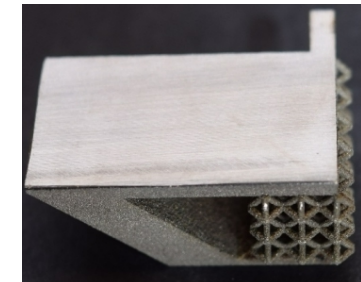


Remove from build plate

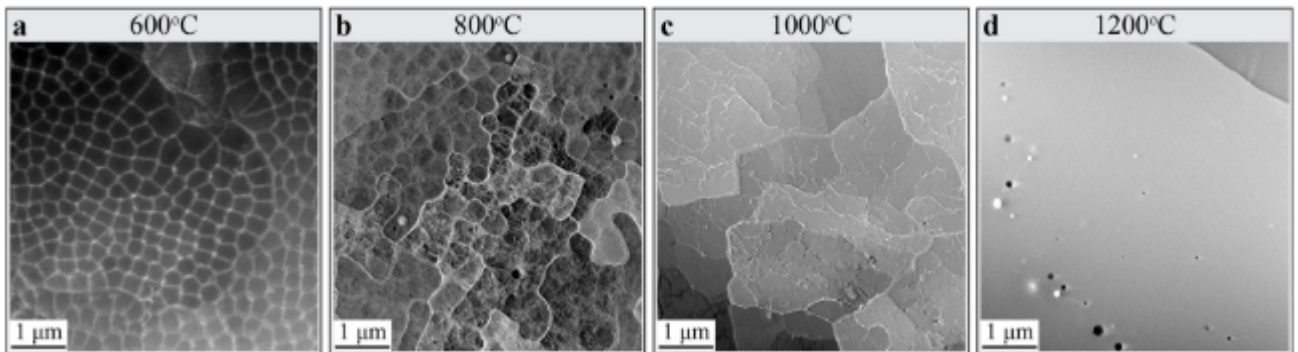
Wire EDM with Brass wire



Bandsaw cut

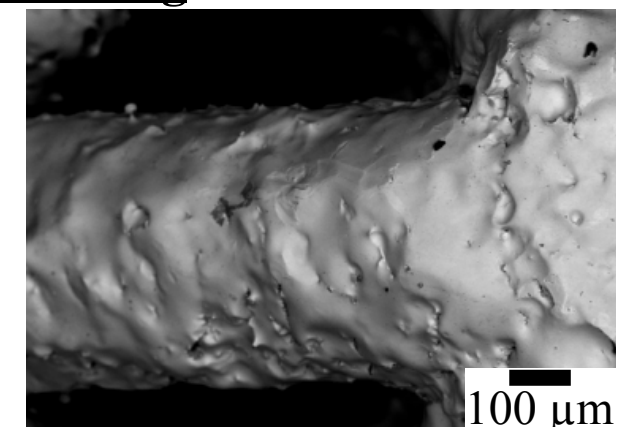
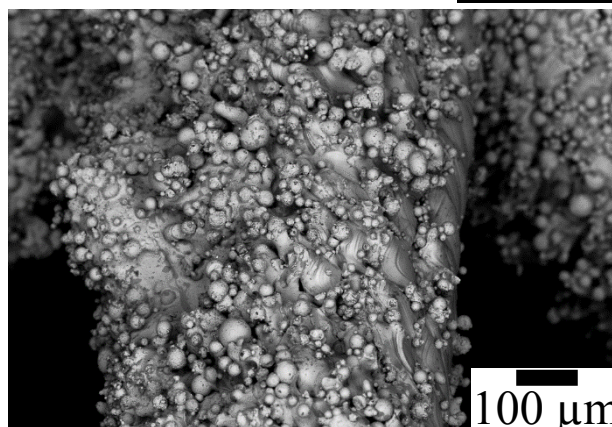


Heat treatments



T. Voisin et al. Acta Materialia (2021)

Surface finishing



Process flow map for metal AM component



Component design/optimization

- Topology optimization
- Improve functionality/product reliability
- Reduced cost/material waste

Material choice/development

- Improved properties
- Reduce constraints

Process

- Select manufacturing technique
- Process optimization
- Print components

Post processing

- Remove components from build plate
- Stress relief
- Machining/surface finishing

Quality assurance

- Specification and standards testing & failure analysis
- Reduced risk

October 15, 2021

<https://www.metal-am.com/wohlers-releases-report-on-post-processing-of-am-parts/>

Many could benefit from using AM metals in their as-printed state:

- Reduces costs
- Reduces lead times
- **Possibly beneficial effects??**

However, there are cases where if you can't remove the as-printed surface, then the AM risk case is elevated to high risk (per NASA-STD-6030), and it is recommended to machine all surfaces.

What will we go over in this talk?



- In-depth characterization of **as-printed** surfaces (LB-PBF 316L).
- Explore corrosion behavior of **as-printed** 316L parts when exposed to the accelerated corrosion test, ASTM G85-A2.

Acknowledgements



Funding: The ACT program, DOD-DOE Joint Munitions Program (JMP), Aging and Lifetime Program.

Many people to thank...

SNL: Kasandra Escarcega-Herrera, Erin Karasz, Jesse Duran, Jason M. Taylor, Rebecca F. Schaller, Jeffrey M. Rodelas, Michael J. Heiden, Bradley H. Jared, Eric J. Schindelholz, Joseph Michael, Paul Kotula, Philip Noell, Daniel Perry, David Saiz, Mark Wilson, Brendan Nation, Joshua Koepke, Christina Profazi, Sara Dickens, Luis Jauregui, Alex Hickman

UVA: Rebecca S. Marshall, Danyil Kovalov, Ryan Katona, Ji Ma, Robert Kelly

LANL: Courtney Clark, Tim Gorey, Jamie Stull, Colt Montgomery, Daniel Hooks

KCNSC: Lucas Rice, Jonathan Dwyer, Andy Deal, Zach Rueger, Francisco Garcia-Moreno

SRNL: Patrick Kuzbary, Savidra Lucatero, Prabhu Ganesan, Hector Colon-Mercado, Paul Korinko

LLNL: Margaret Wu, Seongkoo Cho, Monika M. Biener, Y. Morris Wang, Justin Jones, and S. Roger Qiu, ...

Thanks to the symposium organizers for this opportunity.

Publications on topic:

E.J. Schindelholz, et al., Corrosion of Additively Manufactured Stainless Steels—Process, Structure, Performance: A Review, *Corrosion*, 77 (2021).

M.A. Melia, et al., Marine Atmospheric Corrosion of Additively Manufactured Stainless Steels, *Corrosion*, (2021).

M.A. Melia, et al., How build angle and post-processing impact roughness and corrosion of additively manufactured 316L stainless steel, *npj Materials Degradation*, 4 (2020).

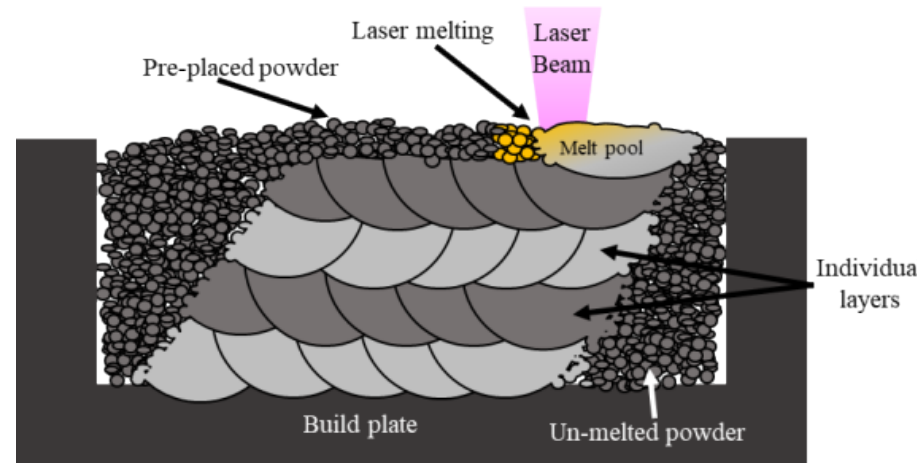
M.A. Melia, et al., Corrosion properties of 304L stainless steel made by directed energy deposition additive manufacturing, *Corros. Sci.*, (2019).

R.F. Schaller, et al., The Role of Microstructure and Surface Finish on the Corrosion of Selective Laser Melted 304L, *J. Electrochem. Soc.*, 165 (2018).

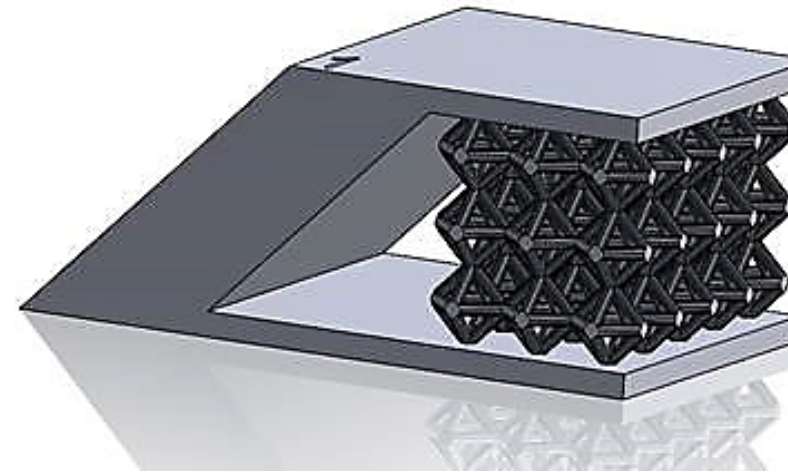
R.F. Schaller, et al., Corrosion Properties of Powder Bed Fusion Additively Manufactured 17-4 PH Stainless Steel, *CORROSION*, 73 (2017).



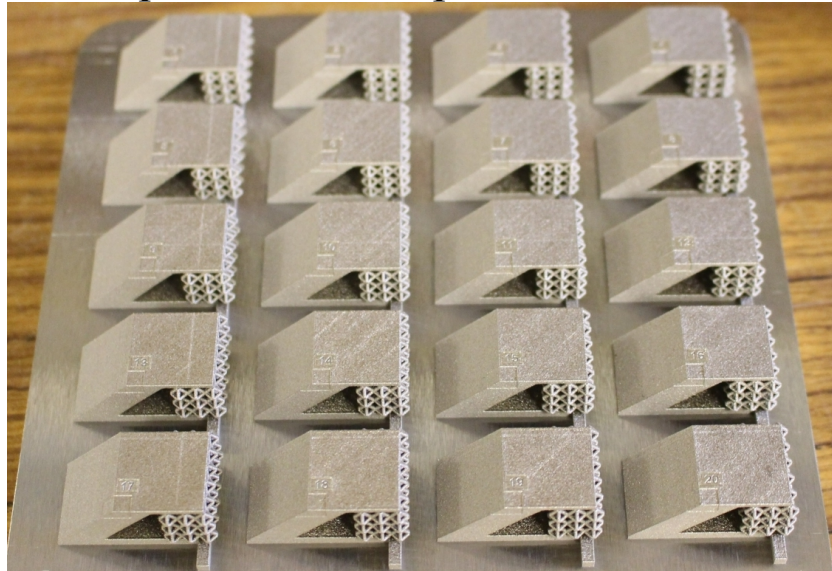
Powder bed fusion 316L samples



Samples were prepared using 316L powder with a powder bed fusion (PBF) technique.

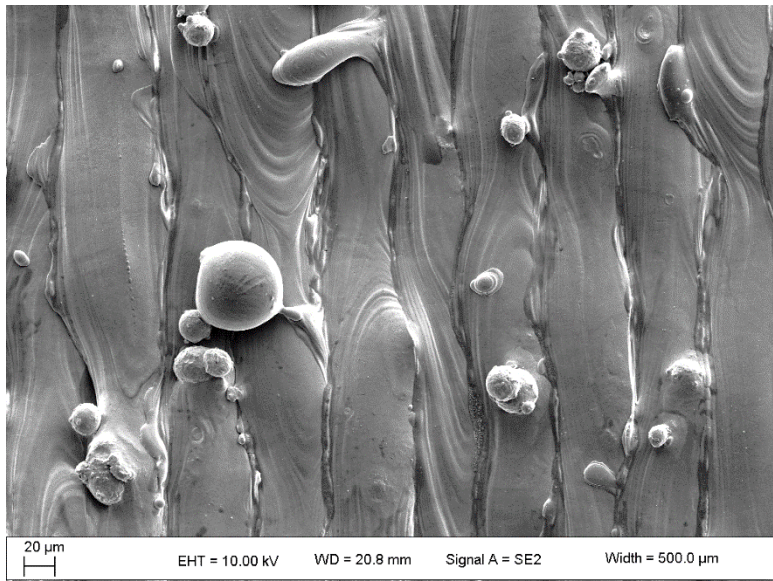


Build plate of 20 samples

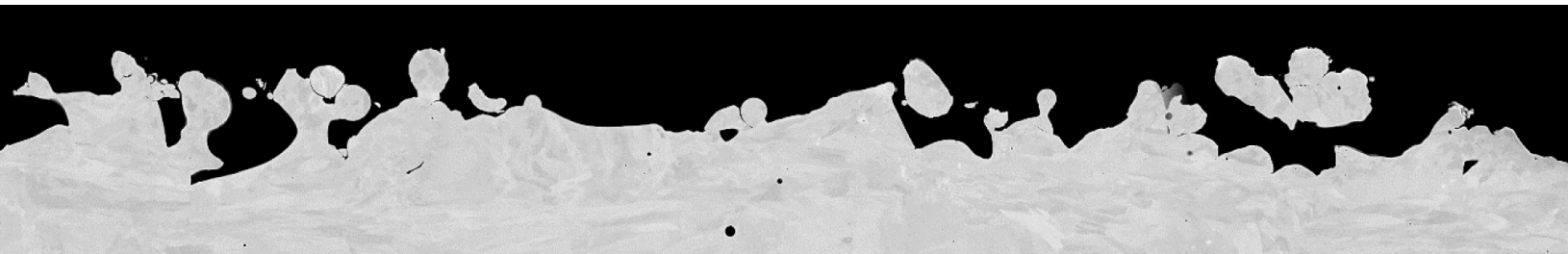
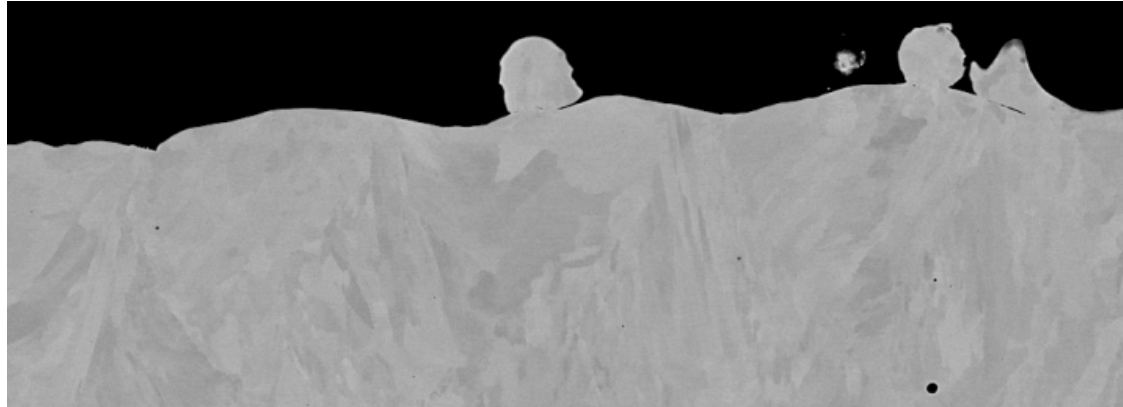


- Samples were printed on 5 different PBF machines, all with the machines optimized parameters for part density.
- SEM images of powder.
- Composition determined by ICP-MS and LECO.
- Powder analysis with laser diffraction.

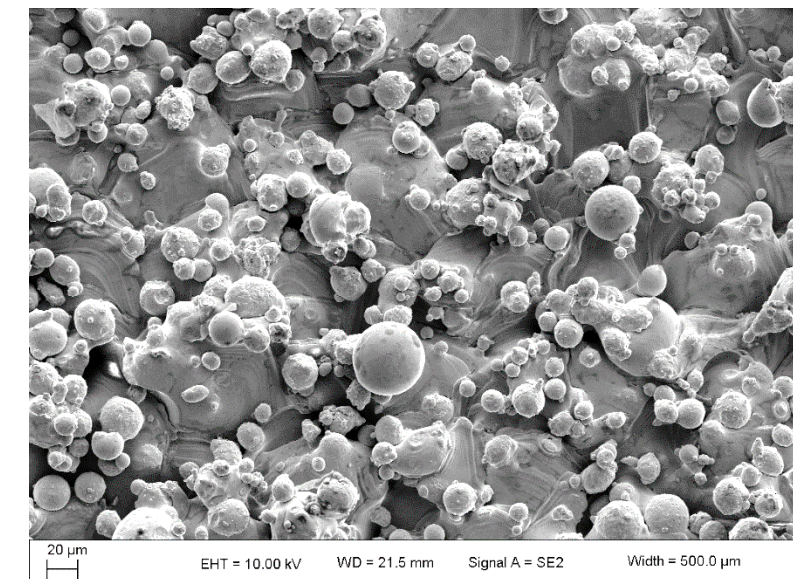
What do as-printed surfaces look like?



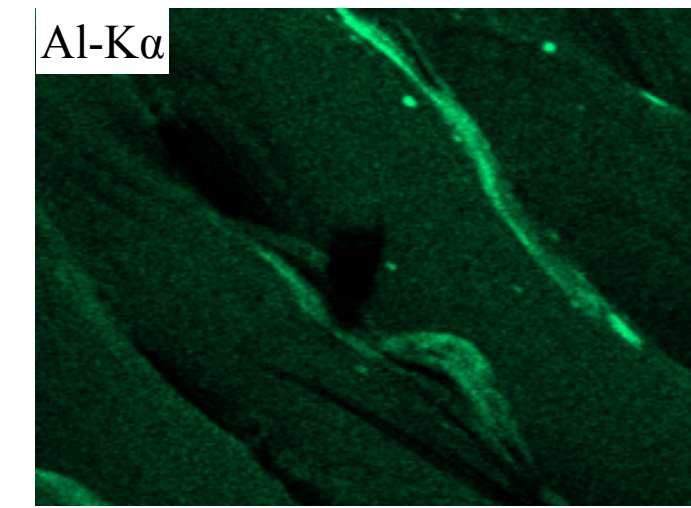
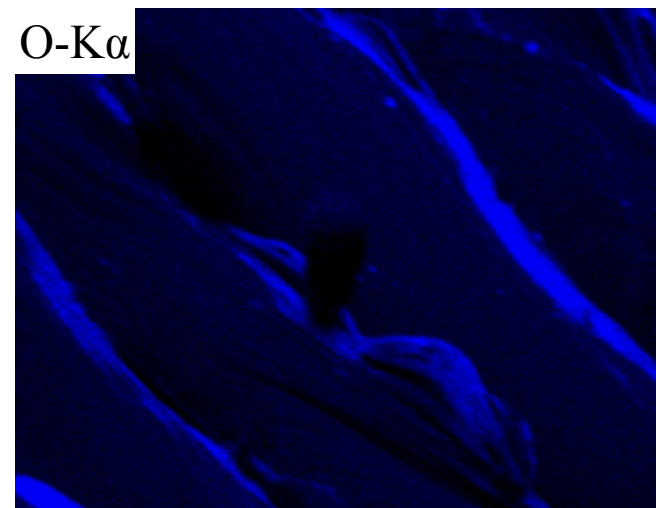
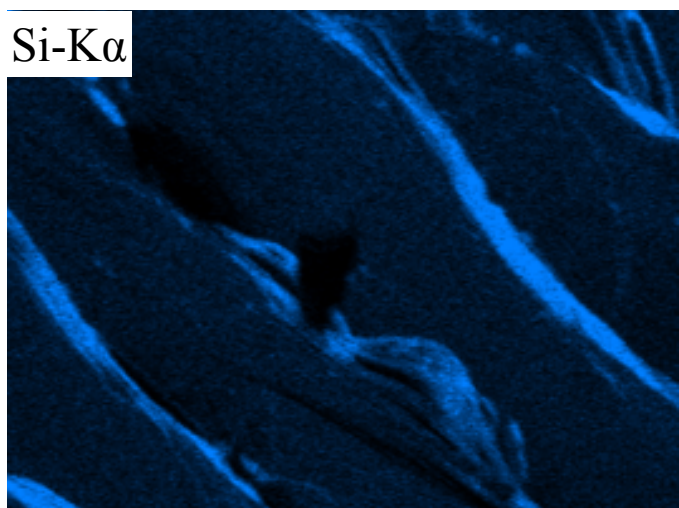
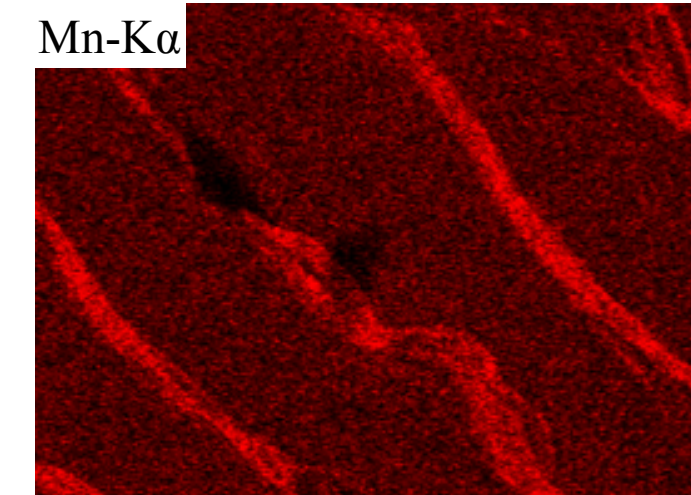
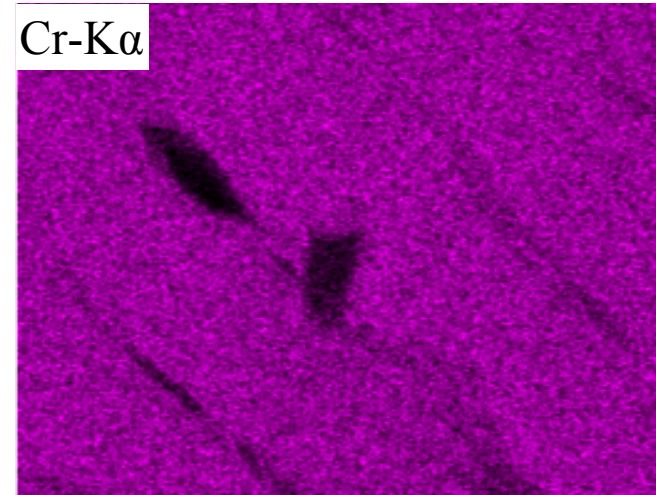
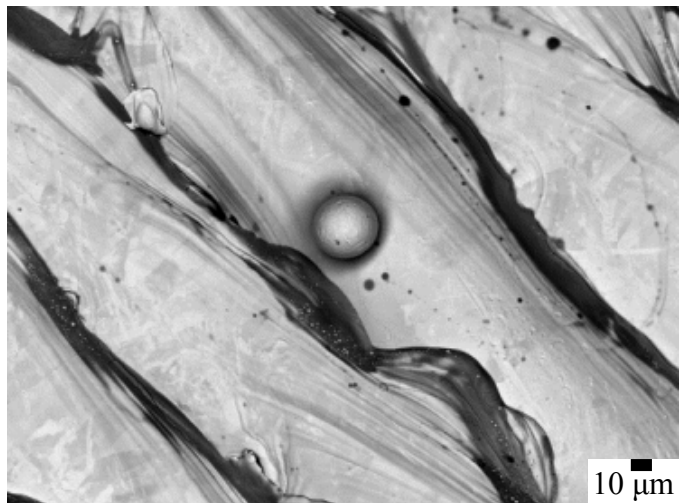
Top surface



Side surface



EDS maps of as-printed top surface



Mechanism for the oxide formation



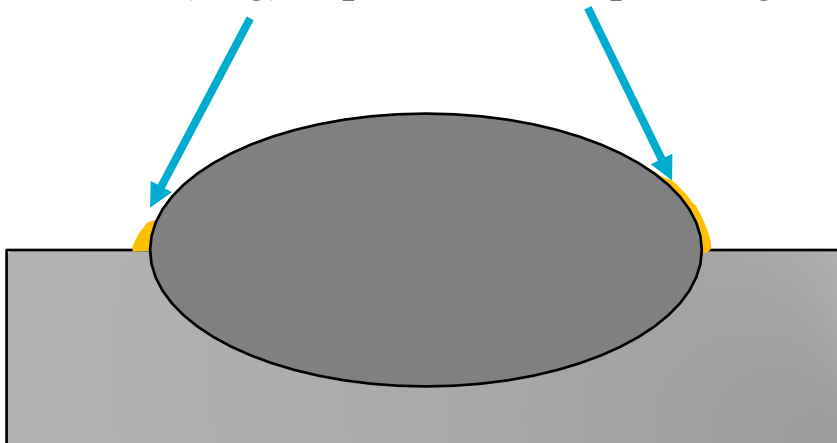
Cold metal transfer – gas metal arc welding



M.R.U. Ahsan, et al., Welding in the World, (2017). (a) Wire 1 (High Si, Mn)

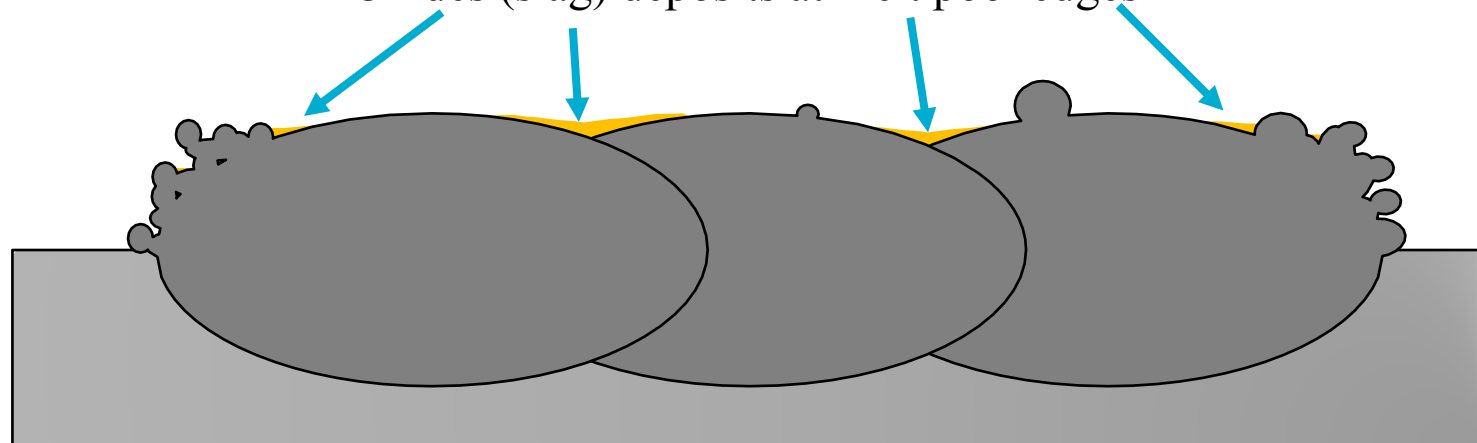
The welding perspective.

Oxides (slag) deposits at melt pool edges



The AM perspective.

Oxides (slag) deposits at melt pool edges



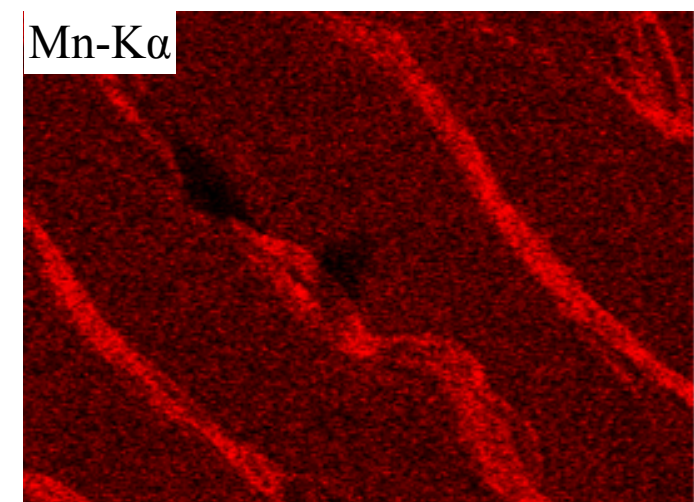
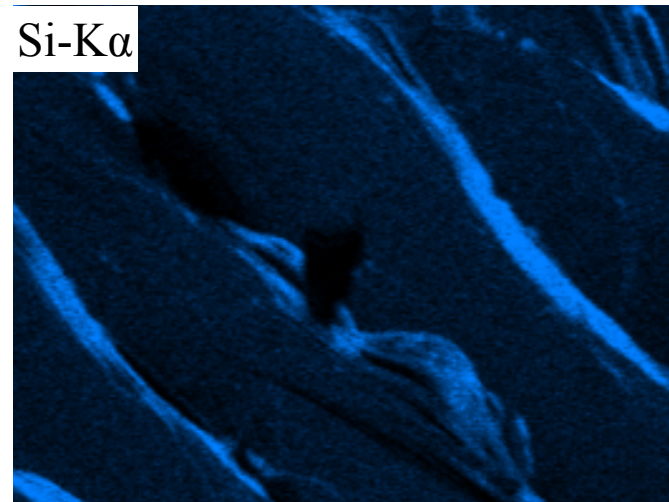
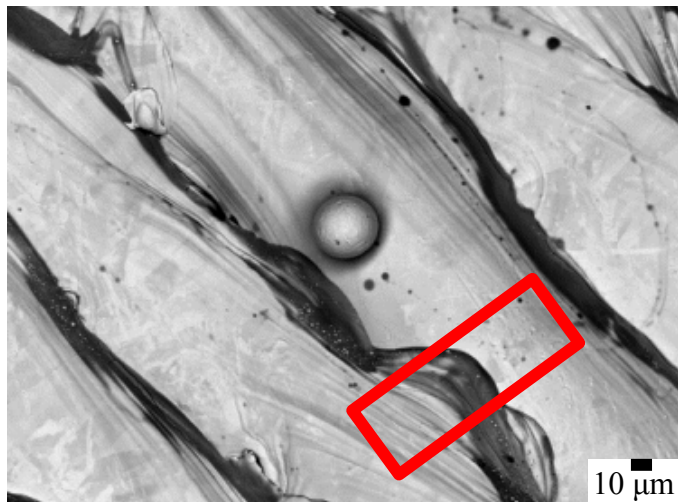
Mechanism for the oxide formation



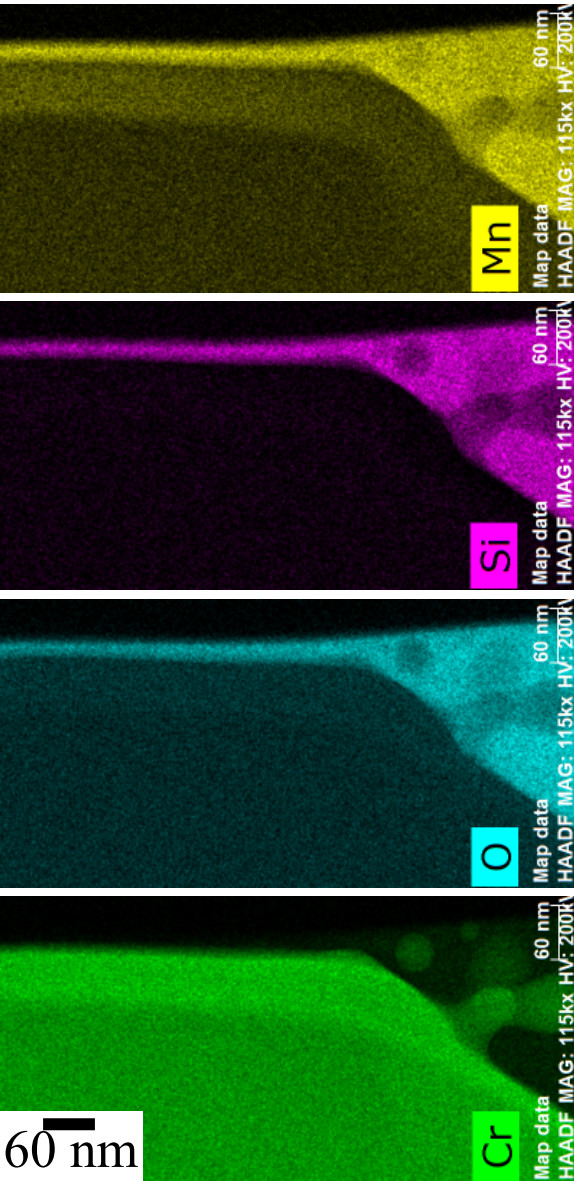
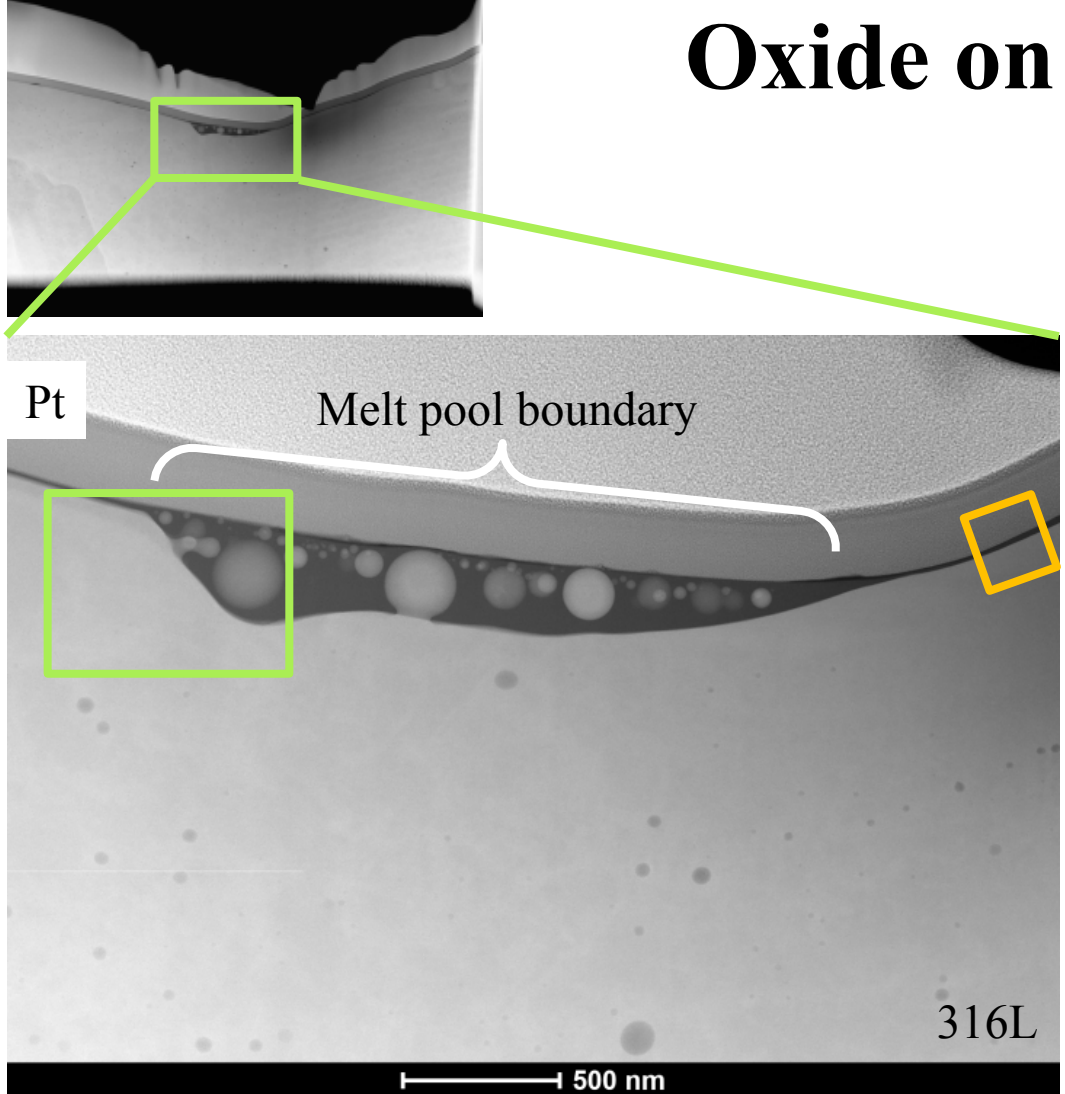
Cold metal transfer – gas metal arc welding



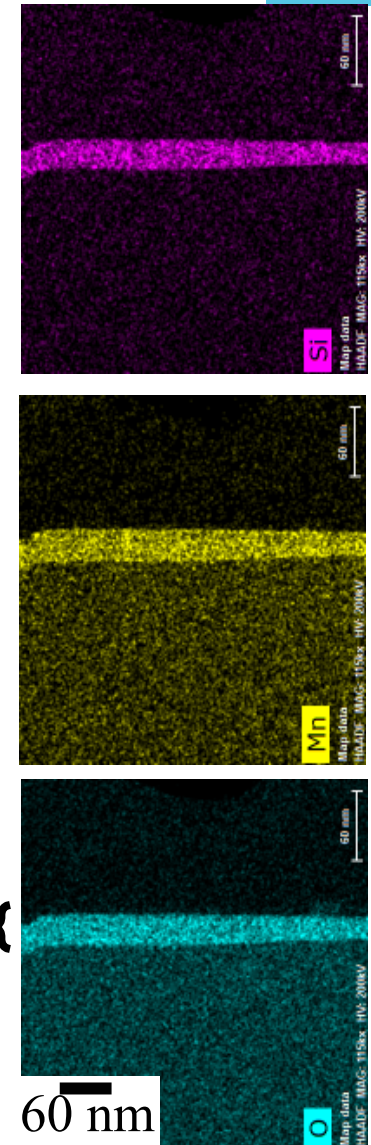
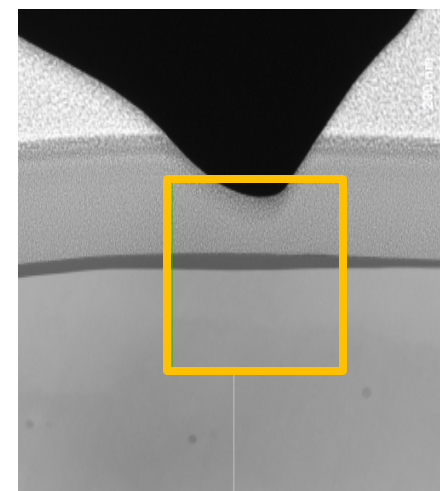
M.R.U. Ahsan, et al., Welding in the World, (2017). (a) Wire 1 (High Si, Mn)



Oxide on PBF 316L surface



To the right
of boundary



~25 nm {

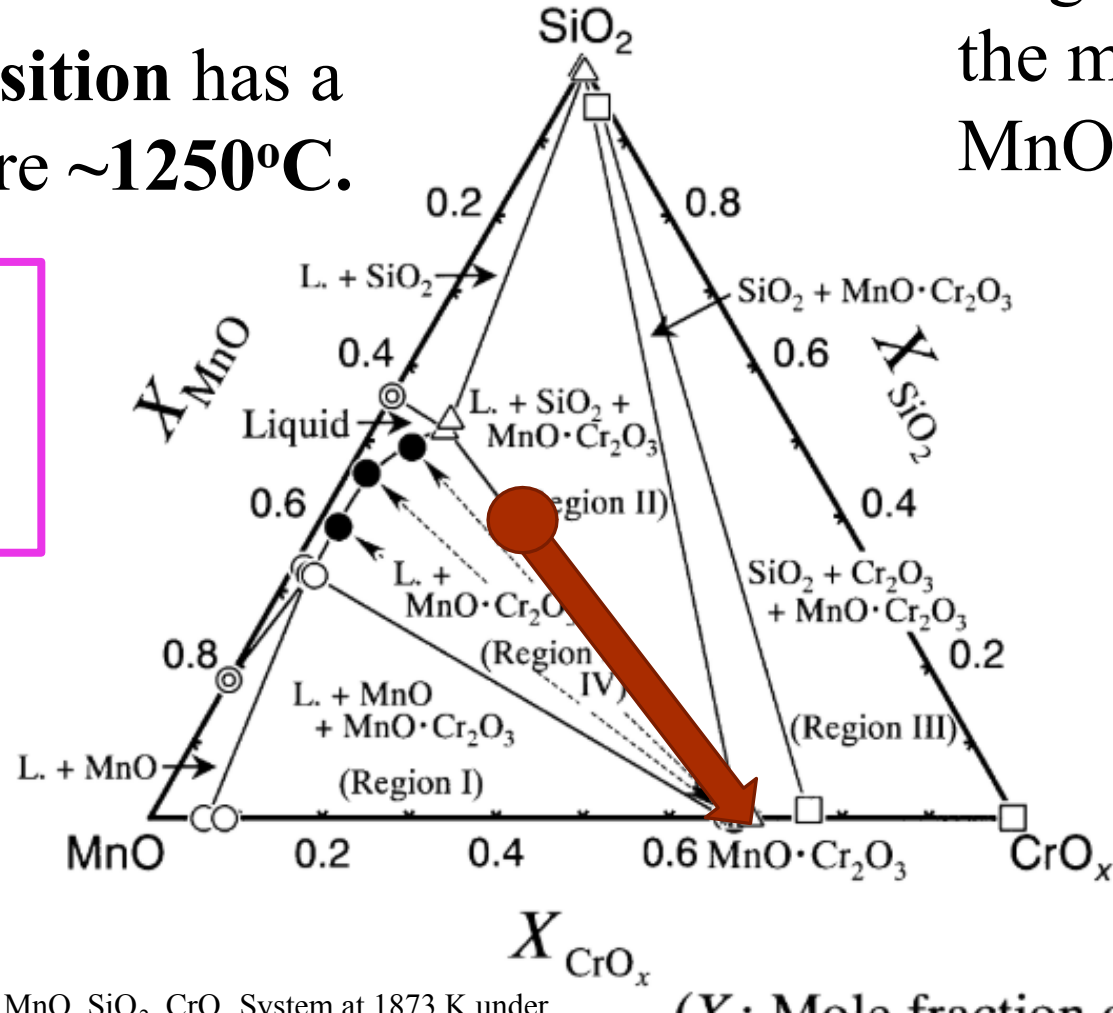
How and why do these oxides form?



- ◎ Liquidus compositions at 1873 K in the MnO-SiO_2 binary phase diagram²⁾

This **oxide composition** has a melting temperature $\sim 1250^\circ\text{C}$.

23% Cr
38% Mn
36% Si



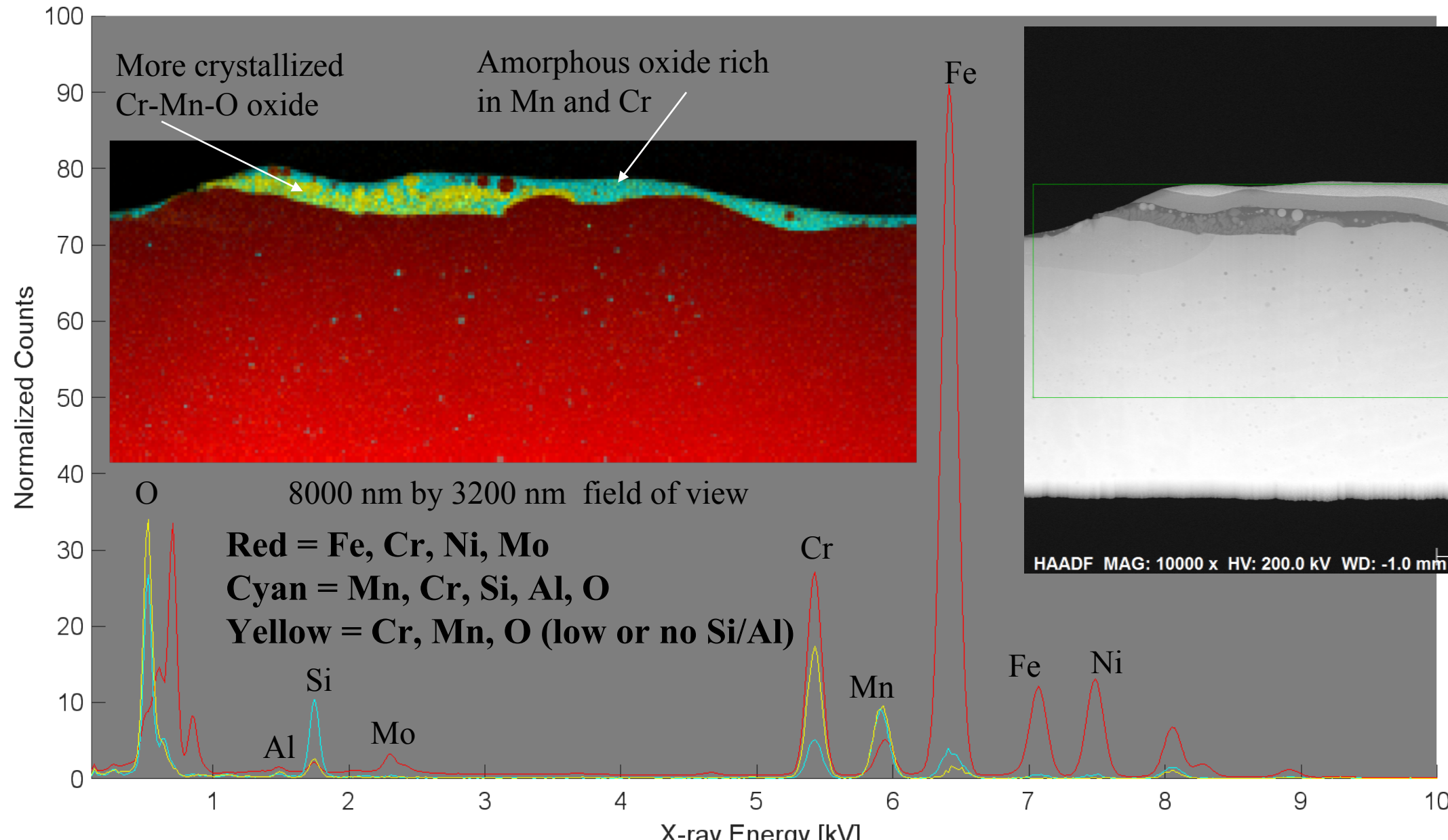
Ternary isotherm phase diagram at 1600°C which is the melting temperature of $\text{MnO}\cdot\text{Cr}_2\text{O}_3$.

Melting temperature of 316L is $\sim 1350^\circ\text{C}$.

Formation of Mn/Cr rich oxide



16

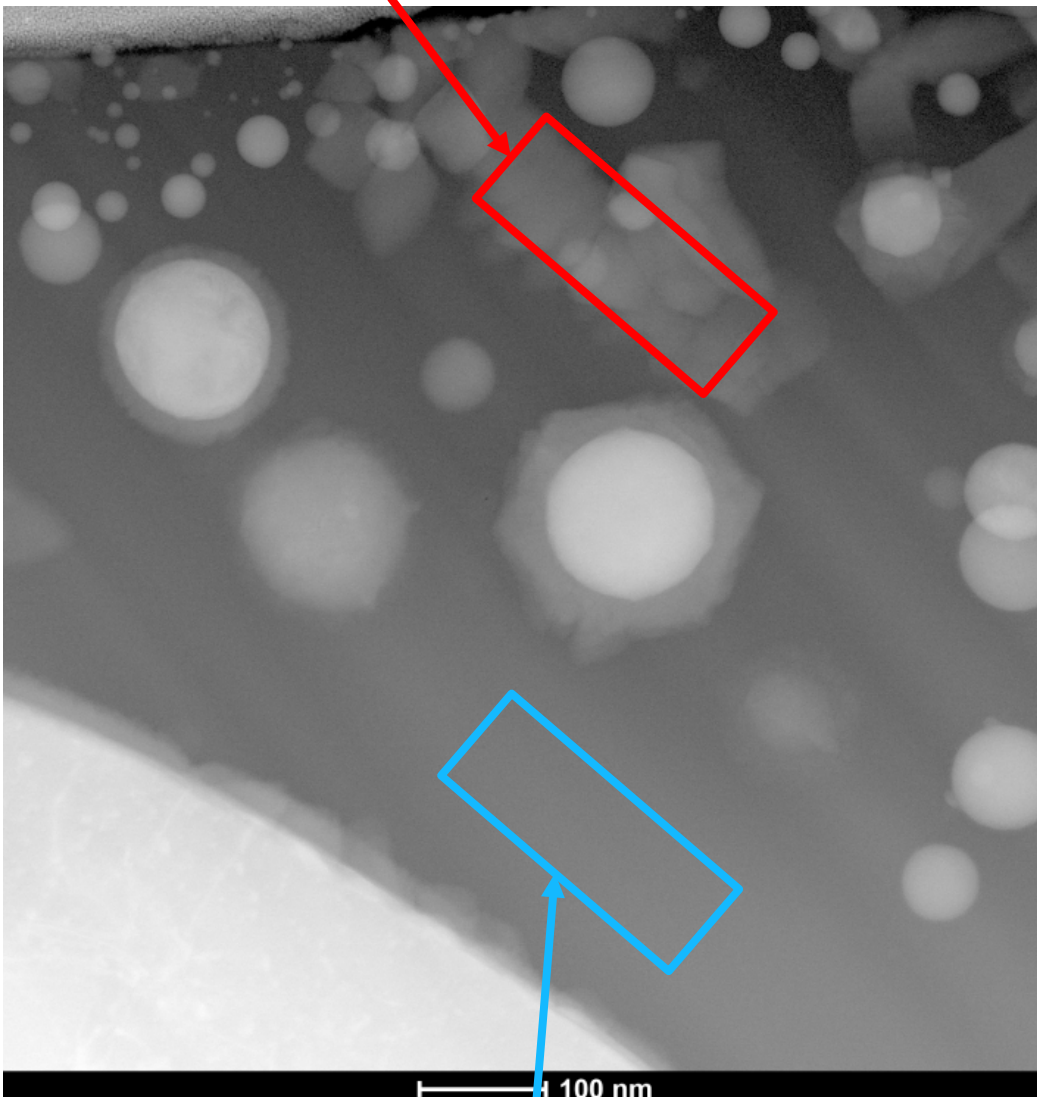


How and why do these oxides form?

17

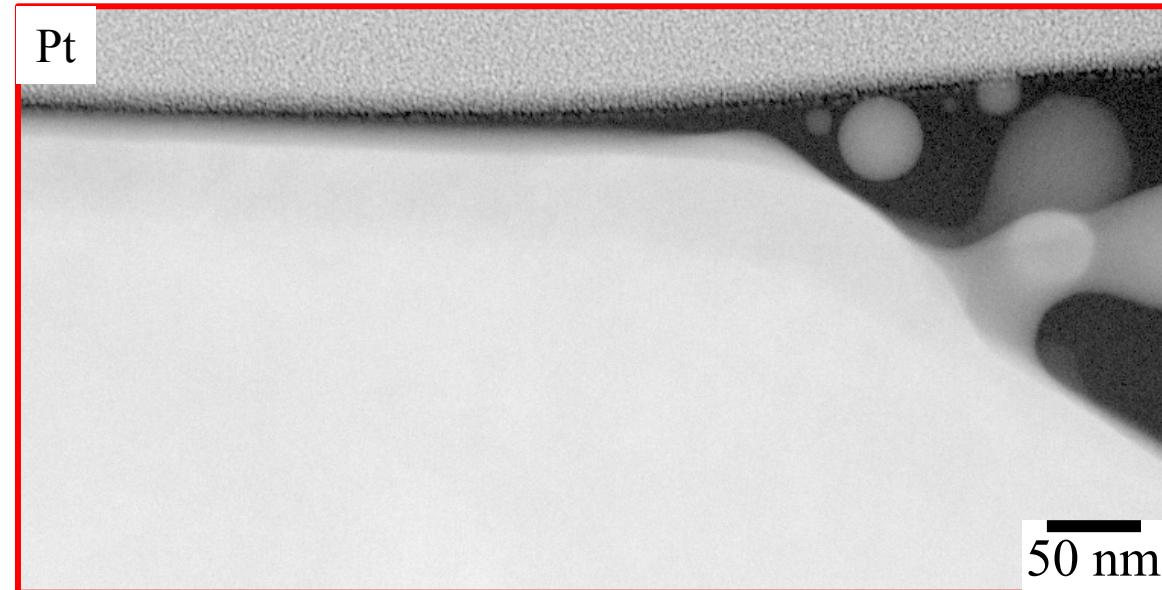
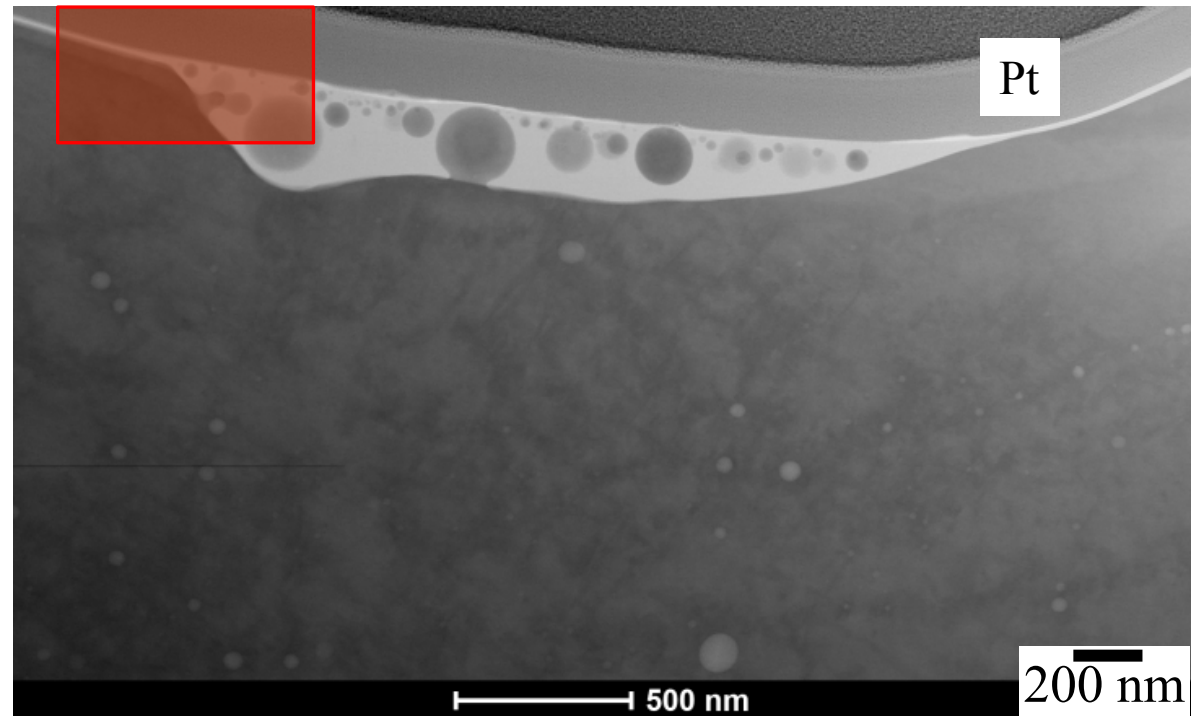


70% Cr-30% Mn oxide



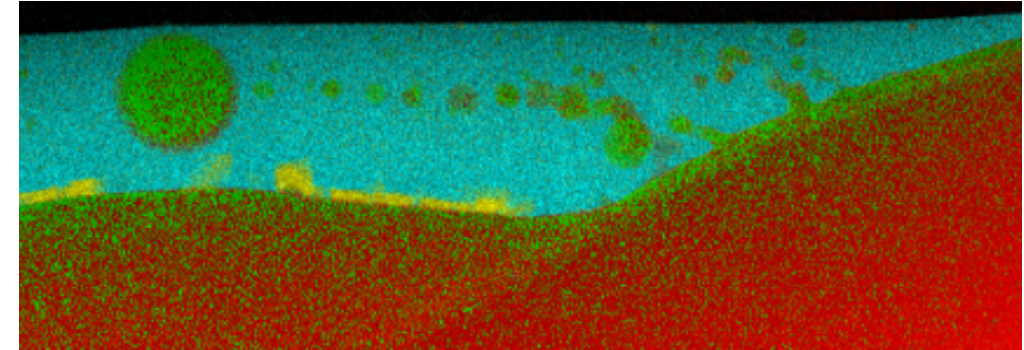
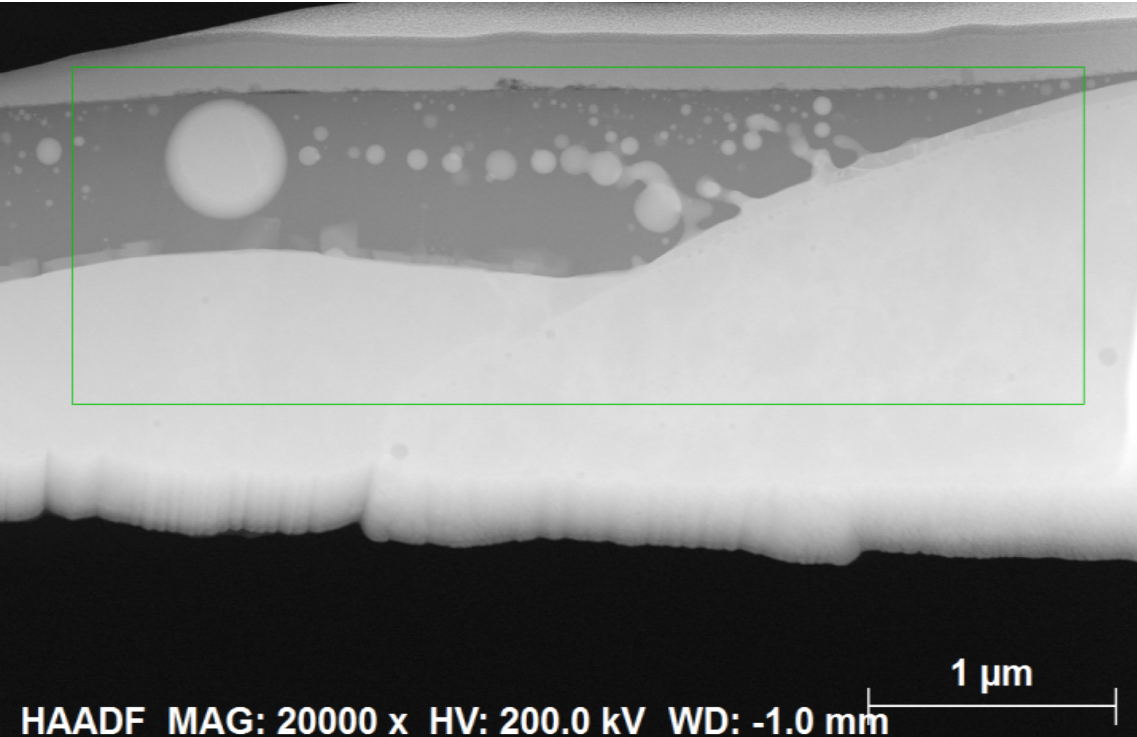
23% Cr-38% Mn-36% Si-3% Al
(UUR)

Oxide on PBF 316L surface



Oxides on 316L surface from SLM280

19



Red = Fe, Cr, Ni, Mn, Mo

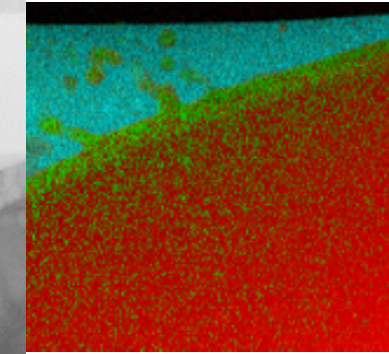
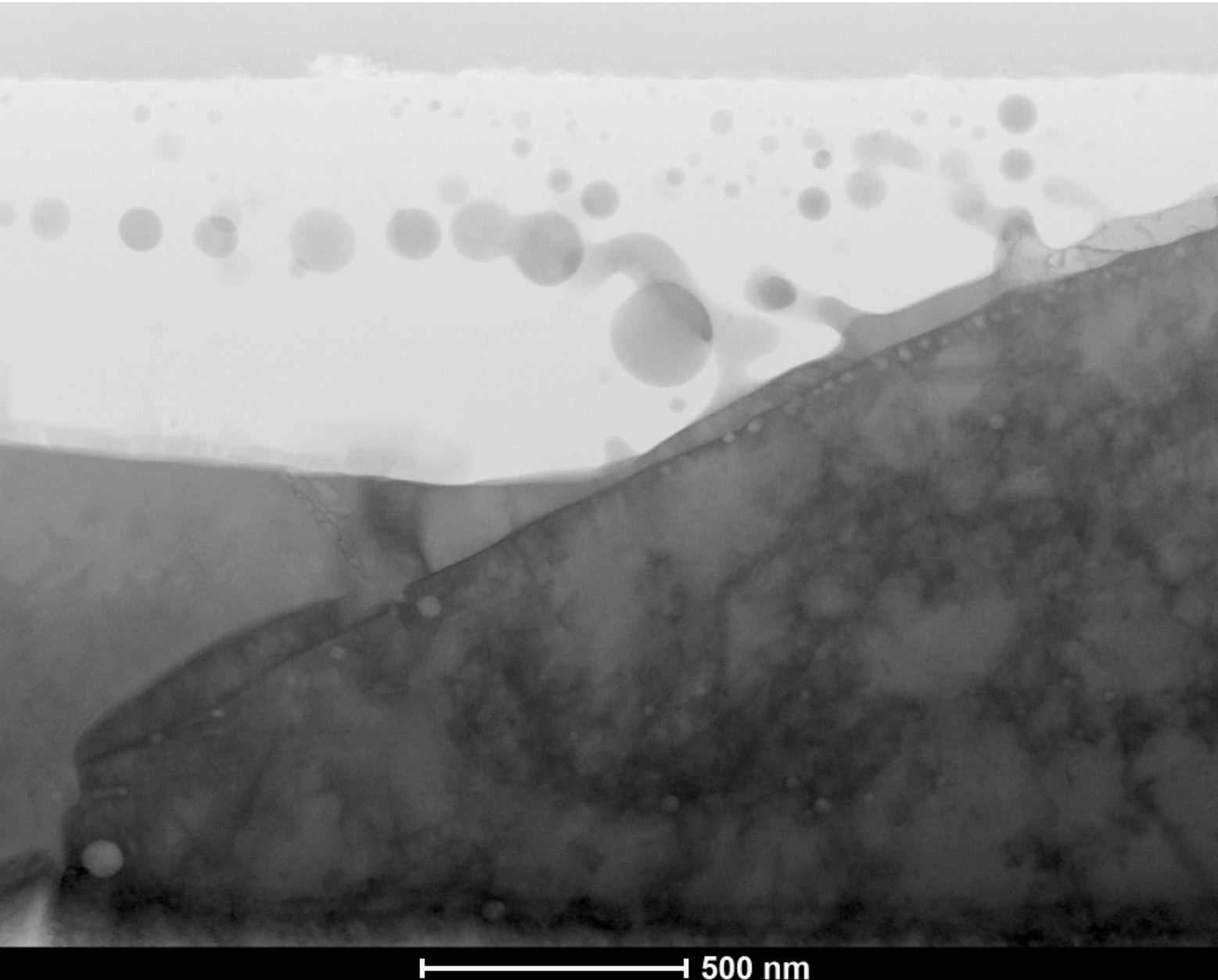
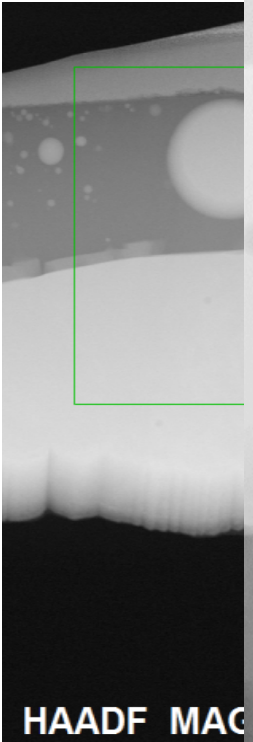
Green (Yellow) = Cr enriched

Cyan = Mn, Cr, Si, Ti, Ca, Al, O

Yellow = Cr, Mn, Ti, Si, Al, O

Oxides on 316L surface from SLM280

20



The as-printed surface of 316L stainless steel



- The oxide on the surface primarily forms via a slag formation mechanism.
 - Lower density oxides (primarily Mn/Si/Cr/Al rich) float to the surface of the liquid melt pool, agglomerate, and deposit at the melt pool edge. (All phases can be in liquid state during this).
- The oxide is an amorphous Mn Silicate, enriched in Cr (melting temp $\sim 1250^{\circ}\text{C}$).
 - A crystalline phase rich in Cr/Mn (minimal Si/Al) should form at equilibrium in the Mn Silicate liquid with a melting temperature of 1600°C .
 - Cr/Mn rich oxide is only found in some cross-sectioned samples.
- Emulsification process creates spheres of stainless steel metal, “floating” in the amorphous oxide – likely happens when both the metal and Mn Silicate are liquid above 1400°C .

ASTM G85-A2: Sample ID



1st set – ProX200 As-printed

2nd set – ProX200

3rd set – EOS M290 As-printed

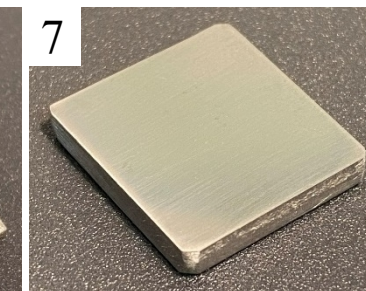
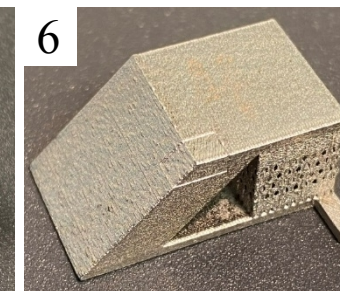
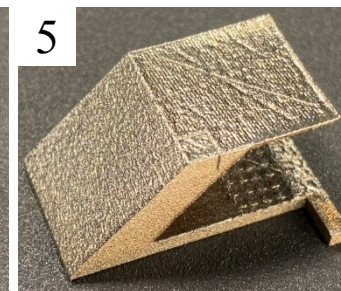
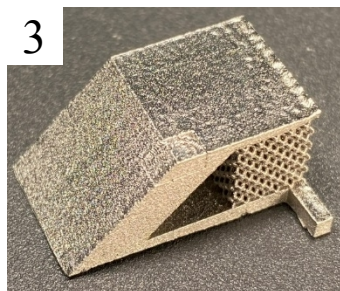
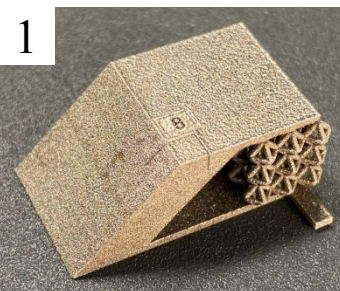
4th set – Renishaw AM250 As-printed

5th set – SLM280 As-printed

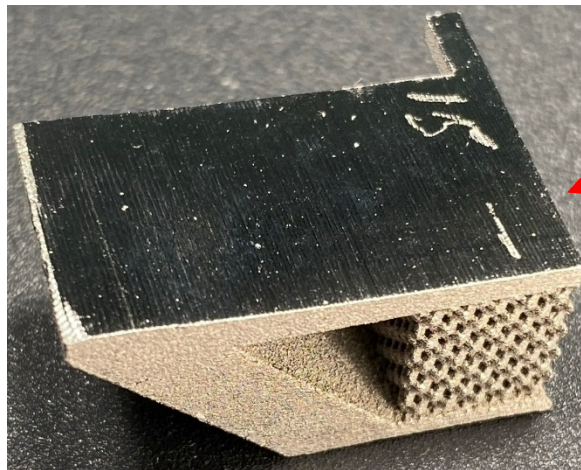
6th set – Concept Laser M2 As-printed

7th set – Wrought 316L

- *wire EDM cut surface*
- *Electropolished*
- *Bandsaw cut surface*
- *Polished with 600 grit sand paper*
- *wire EDM cut surface*
- *Bandsaw cut surface*
- *Fine grinding with 600 grit sand paper*



ASTM G85-A2: Sample ID

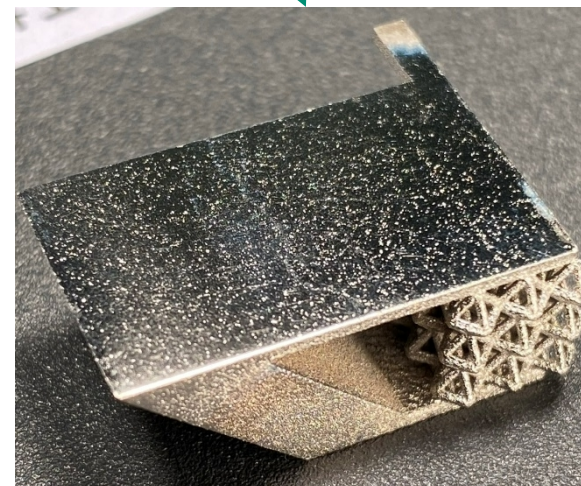
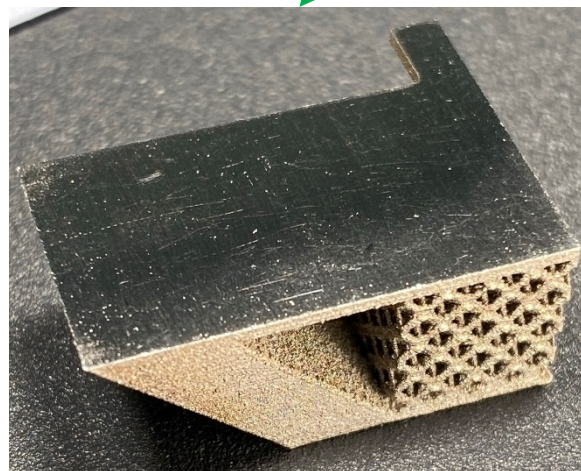


As-cut Bandsaw

As-cut wire EDM

Electropolishing

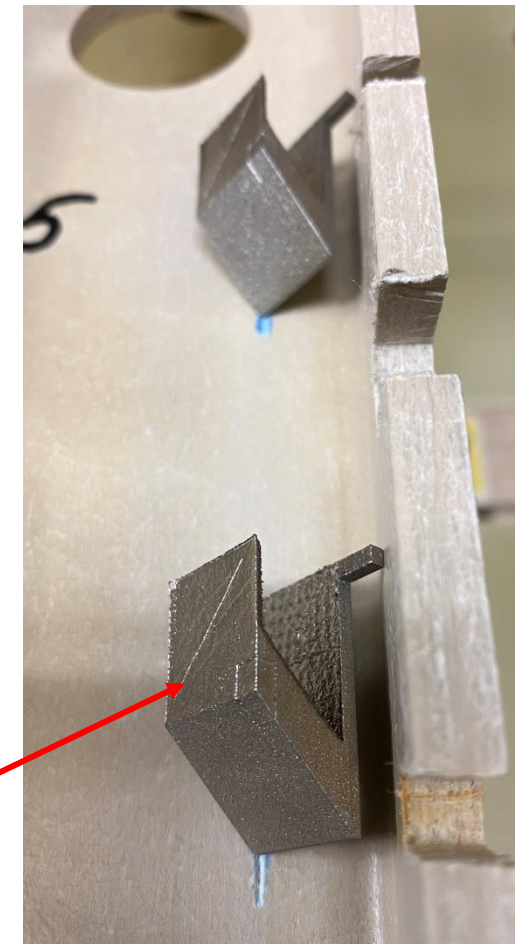
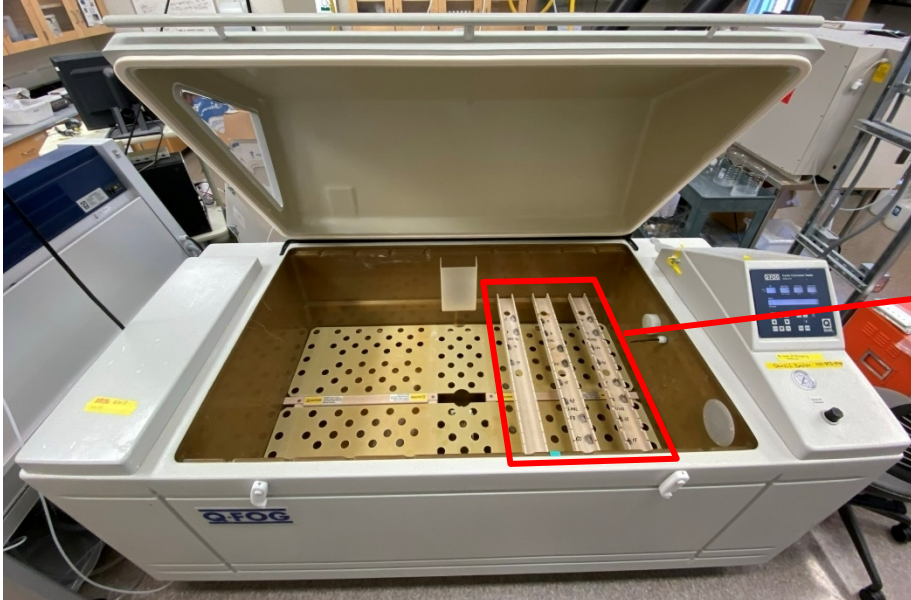
Planar grinding



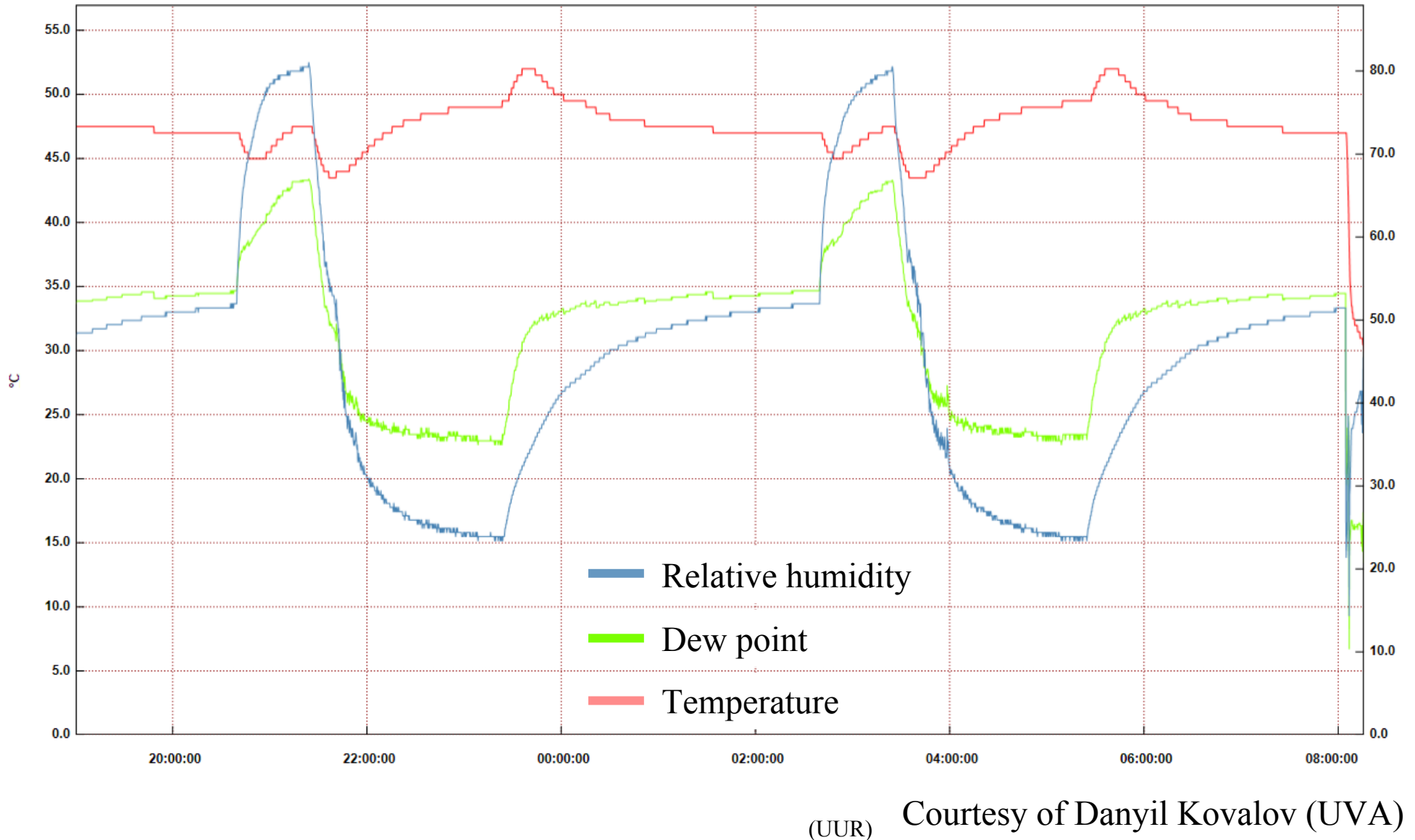
ASTM G85-A2: Setup



- **ASTM for sample testing: G85 A2 with wet bottom**
 - Equipment: Q-fog cyclic corrosion tester.
 - Solution: 0.9M NaCl acidified to pH 3 with acetic acid.
 - Test temperature: 49°C.
 - Duration: 2000 hr.
 - Sample holder: PEEK rack with milled paths to place AM 316 samples.



ASTM G85-A2: RH and Temp.



Samples after 2000 hours – Top down



ProX 200
As-printed



ProX 200
Electropolish



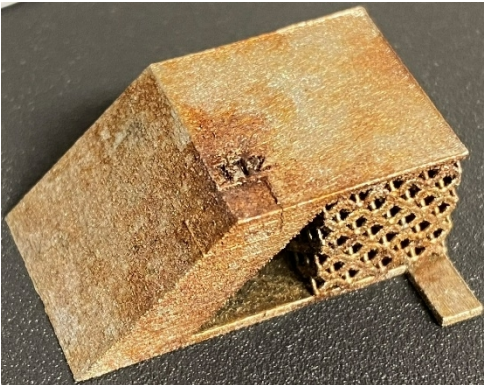
EOS M290
As-printed



Wrought surface
was polished



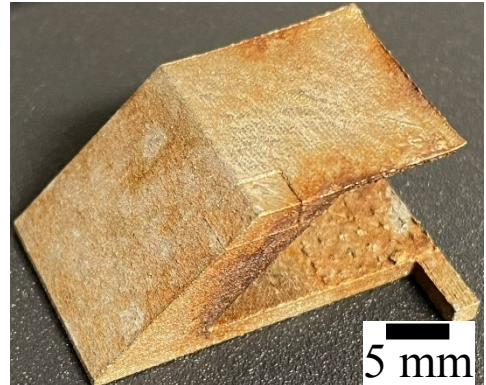
Renishaw
As-printed



Concept M2
As-printed



SLM®280
As-printed



5 mm

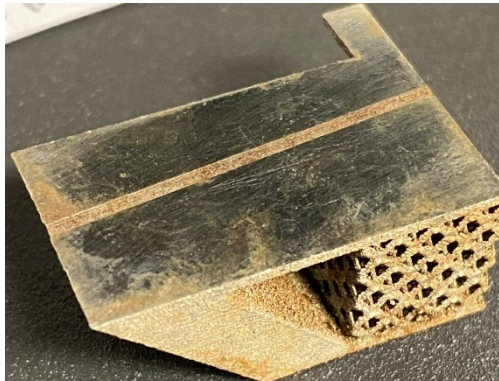
Samples after 2000 hours – Cut surface



ProX 200
As-printed



Renishaw
As-printed



ProX 200
Electropolish



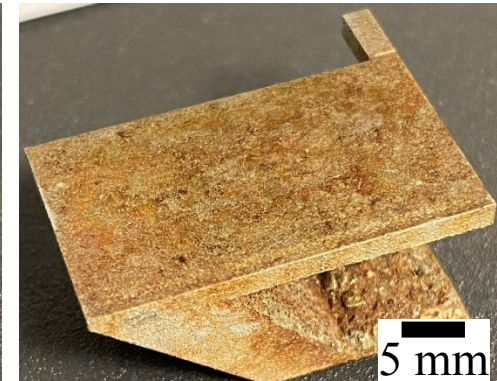
Concept M2
As-printed



EOS M290
As-printed



SLM®280
As-printed



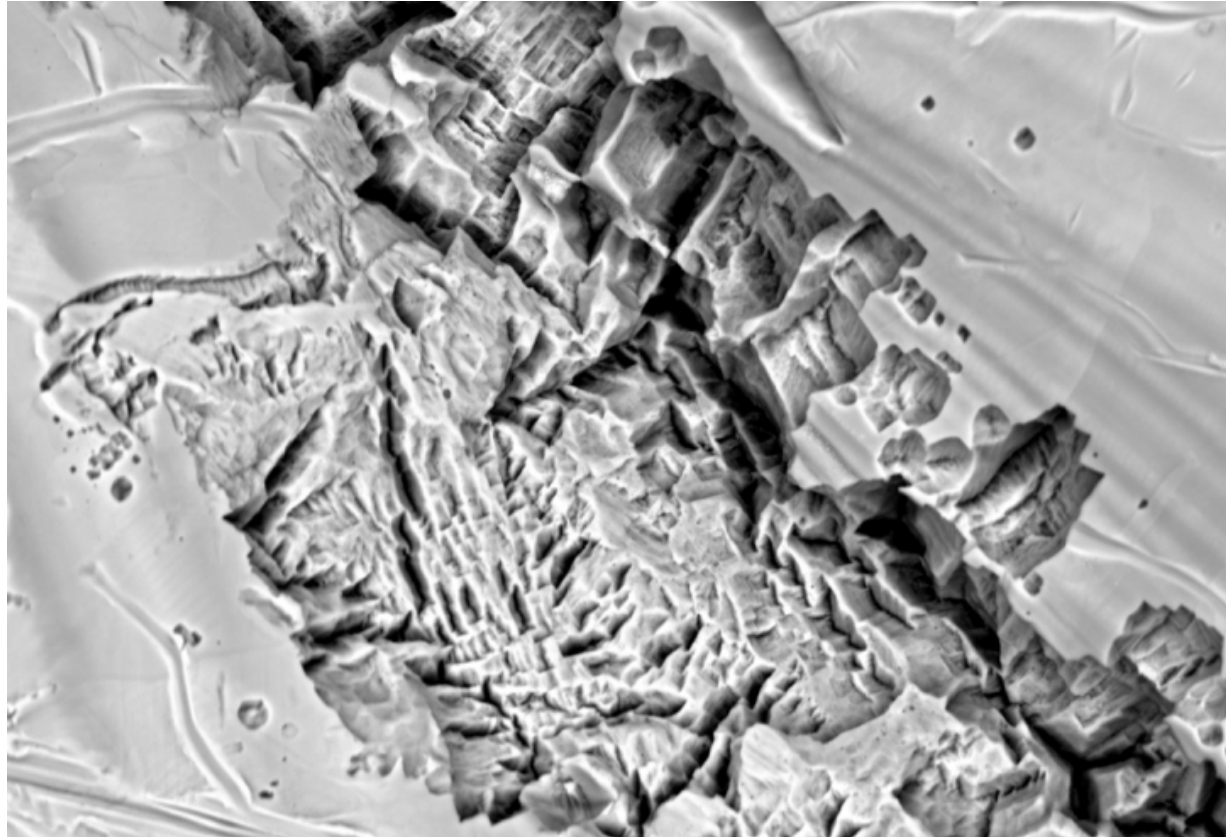
Wrought surface
was polished



Pit morphology

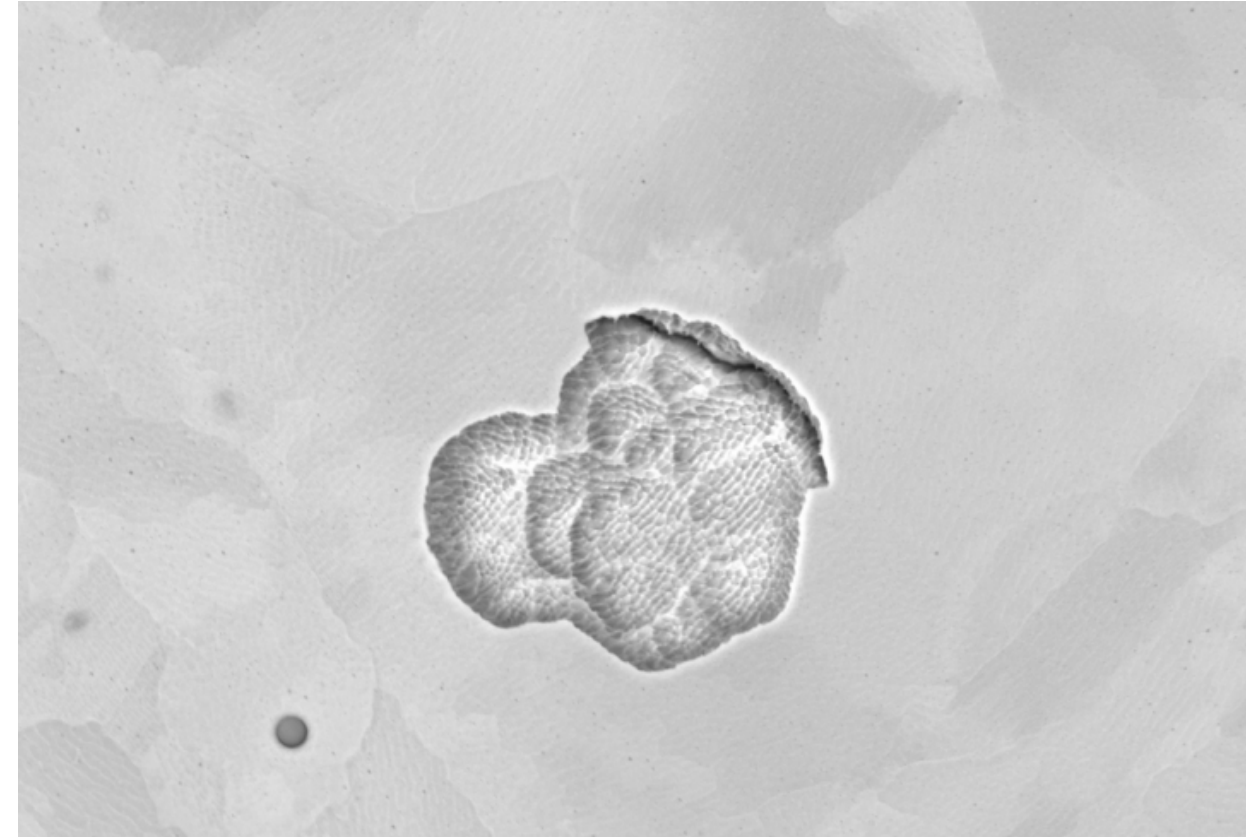


ProX 200
As-printed



EHT = 15.00 kV WD = 8.6 mm Signal A = BSD Width = 50.00 μ m

ProX 200
Electropolish

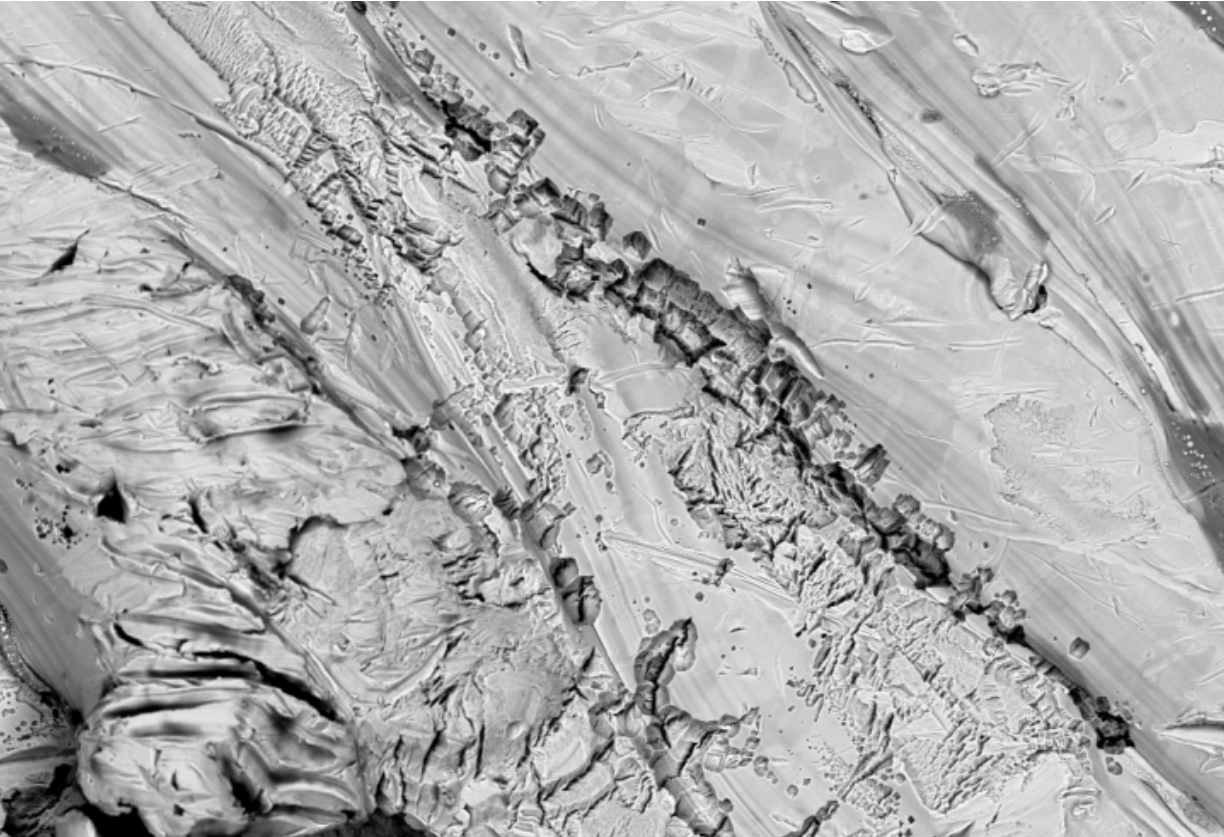


EHT = 15.00 kV WD = 8.8 mm Signal A = BSD Width = 50.00 μ m

Pit morphology

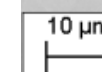
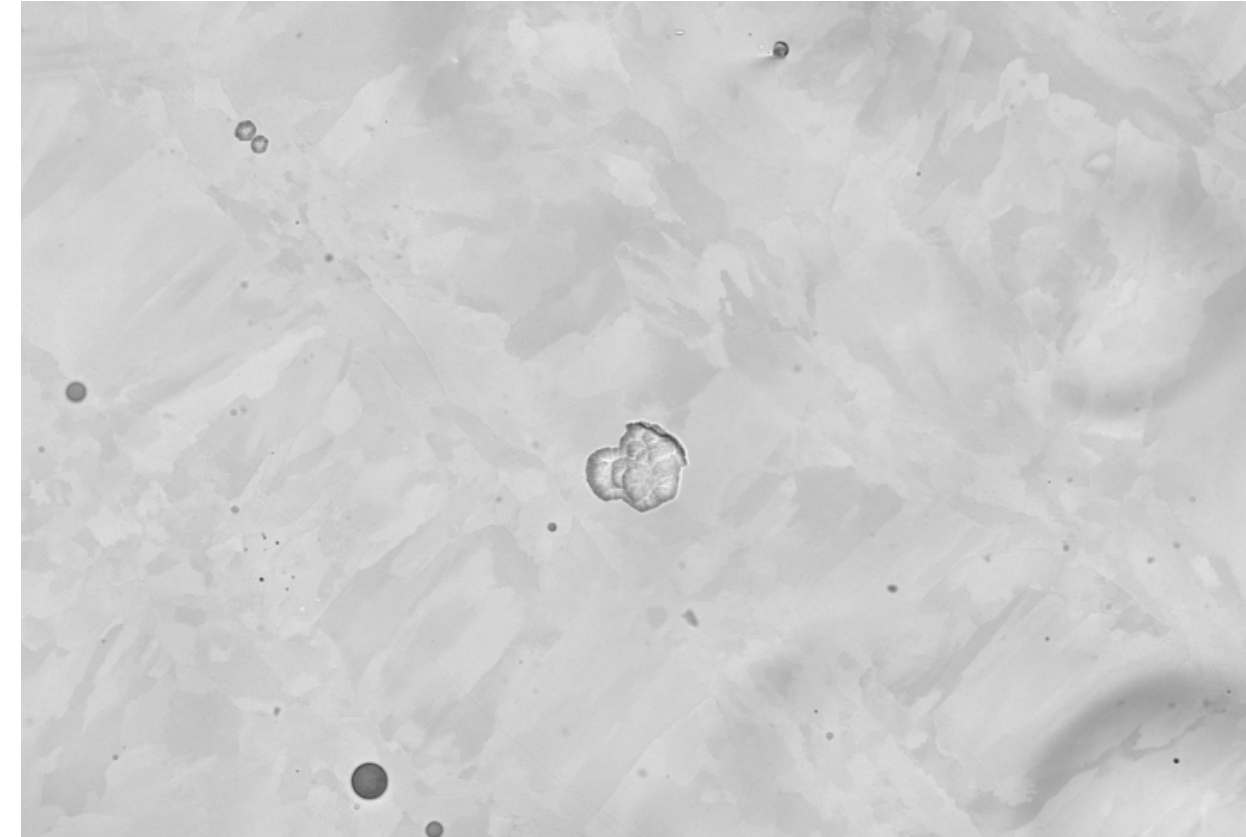


ProX 200
As-printed



EHT = 15.00 kV WD = 8.6 mm Signal A = BSD Width = 200.0 μ m

ProX 200
Electropolish

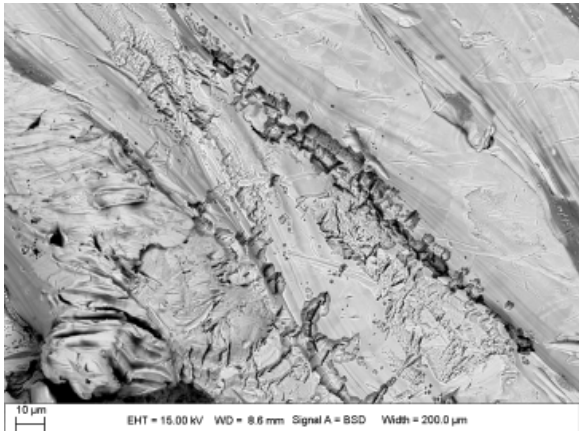


EHT = 15.00 kV WD = 8.8 mm Signal A = BSD Width = 200.0 μ m

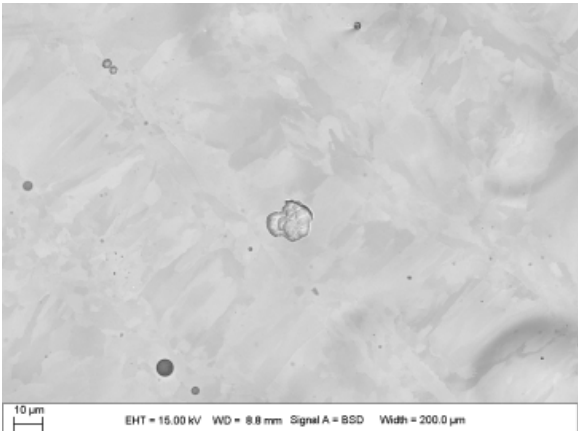
Pit morphology – Top surface



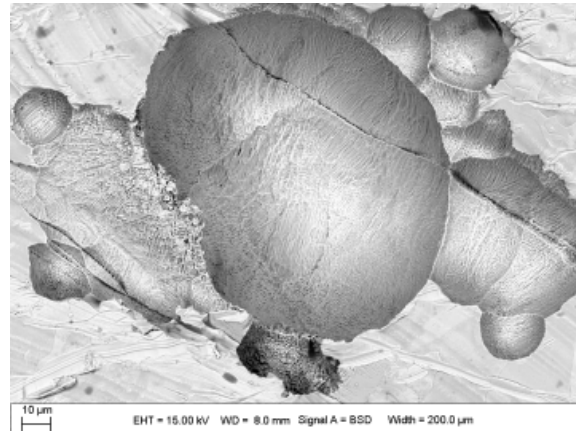
ProX 200
As-printed



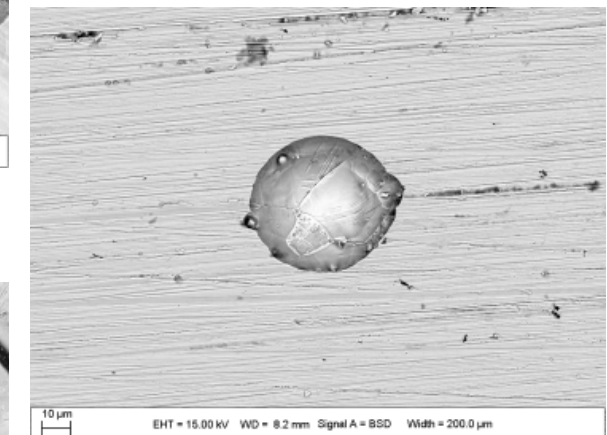
ProX 200
Electropolish



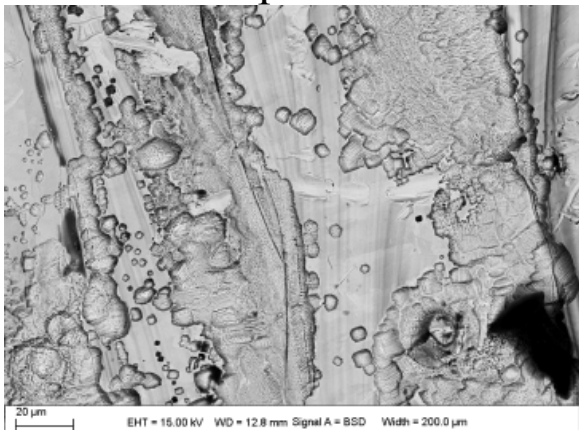
EOS M290
As-printed



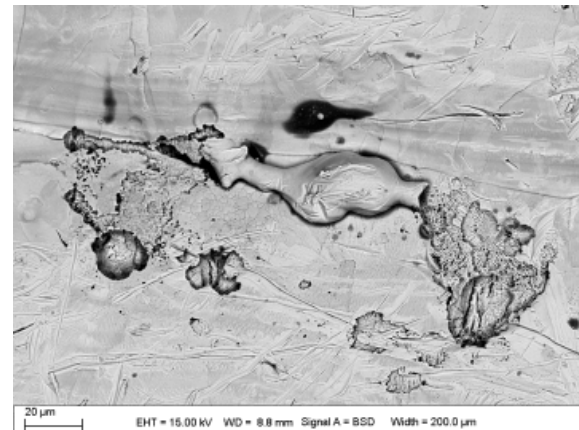
Wrought surface
was polished



Renishaw
As-printed



Concept M2
As-printed



SLM®280
As-printed



ASTM G85-A2 conclusions (so far)



- Wire EDM as-cut surface had the most aggressive corrosion based on optical analysis.
- Electropolished surfaces were least susceptible to corrosion.
- As-printed samples had different quantities of corrosion based on optical, but similar morphology (many pits appeared to initiate from melt pool boundaries).

Current results correlate well with electrochemical experiments (breakdown potential, etc.).

Thank you for your attention!



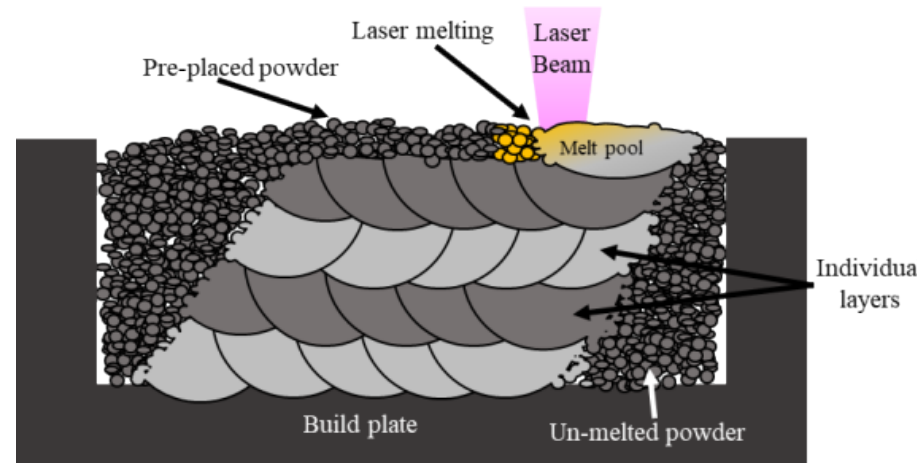
Questions...?

Please contact with questions/comments:

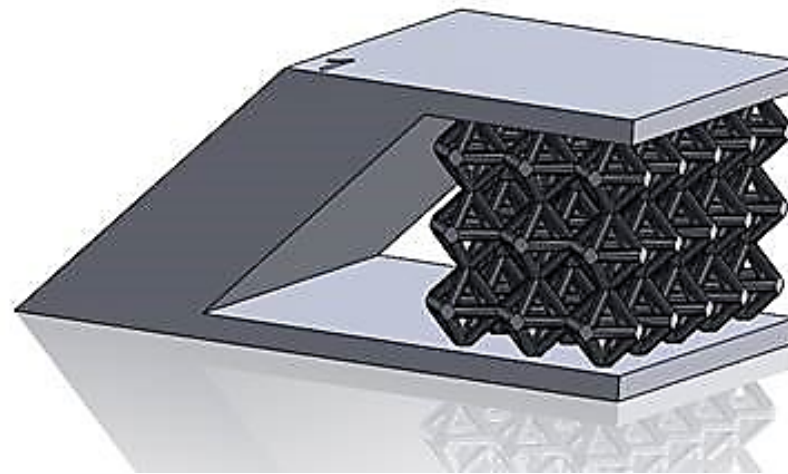
Michael Melia

mamelia@sandia.gov

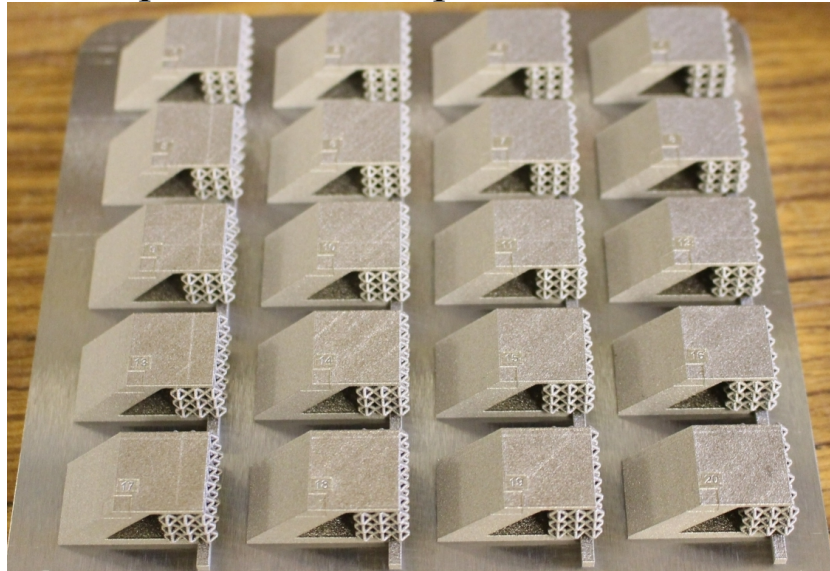
Powder bed fusion 316L samples



Samples were prepared using 316L powder with a powder bed fusion (PBF) technique.



Build plate of 20 samples



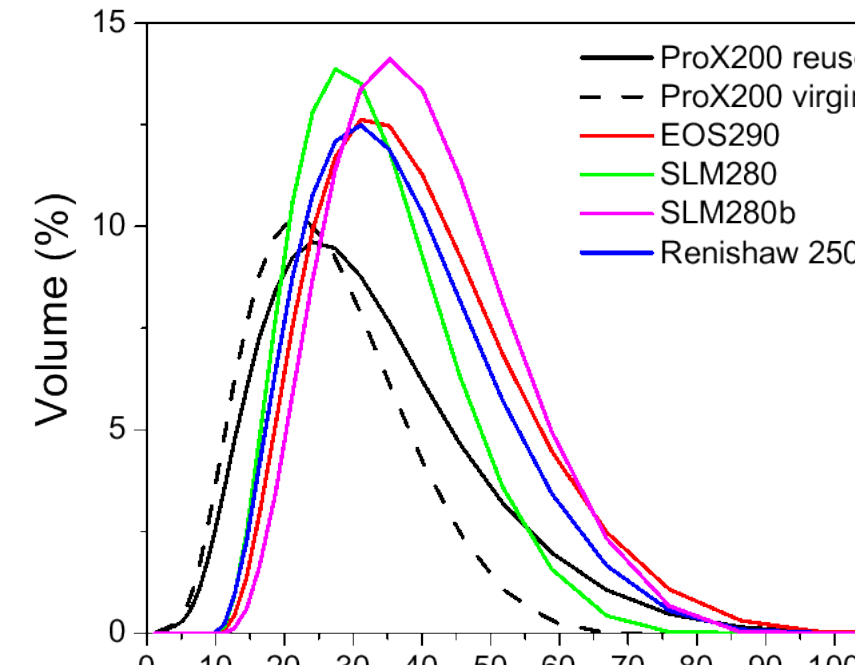
Machine model number	Power (W)	Scanning velocity (mm/s)	VED (J/mm)	Hatch spacing (um)	Layer thickness (um)	Scan pattern
EOS M290	214.2	928.1	57.7	100	40	Stripes
3D Systems ProX DMP200	113	1400	53.8	50	30	Hexagon
Renishaw AM250	200	100	363.6	110	50	Stripes
SLM®280	175	850	57.2	120	30	Stripes
M2 Series 5	300	700	65.9	130	50	Stripes

Powder characterization



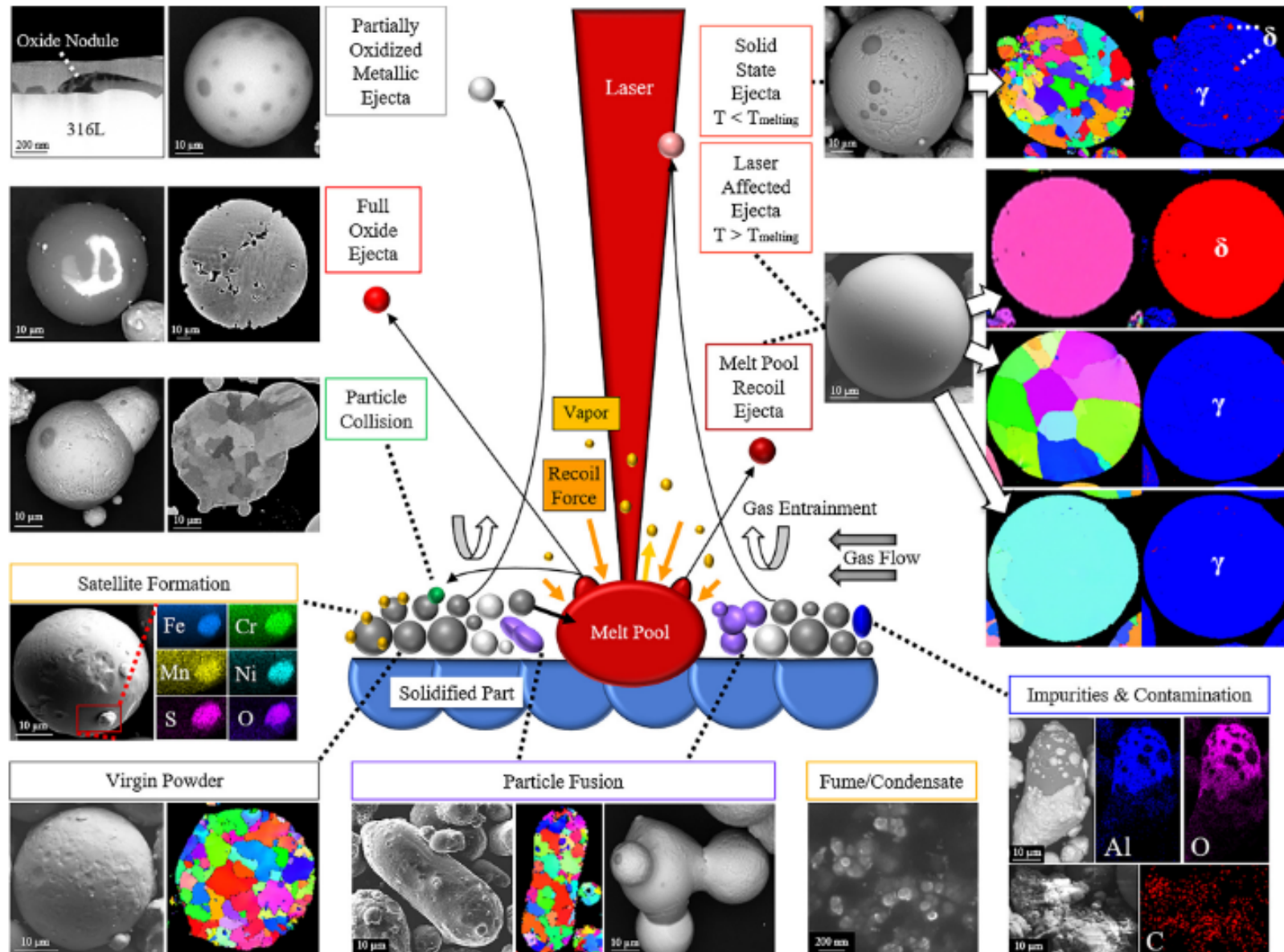
- SEM images of powder.
- Composition determined by ICP-MS and LECO.
- Powder analysis with laser diffraction.

	ProX 200 reused	EOS M290 reused	SLM280 reused	M2 Series 5 Reused	Renishaw reused
Apparent Density (g/cc)	4.25	4.22	3.97	4.16	4.26
ASTM B964 Carney Flow (sec./150 g.)	13	9	9	8	8
Hall Flow ASTM B213 (sec./50 g.)	17	13	14	12	13
Skeletal Density (g/cc)	7.9893	7.9549	7.9891	7.9234	7.9552
Tap Density (g/cc)	5.07	5.02	4.94	5.02	5.14



Wt%	Al	C	Cr	Cu	Fe	Mn	Mo	N	Ni	O	P	S	Si
ProX 200	0.003	0.018	17.12	0.15	67.2	1.28	2.19	0.12	11.18	0.11	0.015	0.013	0.49
EOS M290	0.003	0.024	17.8	0.013	65.5	0.77	2.19	0.099	12.96	0.032	0.005	0.006	0.57
SLM®280	0.006	0.012	16.83	0.11	67.6	1.18	2.24	0.059	11.33	0.055	0.008	0.009	0.43
M2 Series 5	0.007	0.028	17.7	0.026	65.8	0.53	2.24	0.071	12.87	0.03	0.005	0.008	0.55
Renishaw	0.005	0.025	17.12	0.013	66.6	1.08	2.33	0.031	12.13	0.049	0.005	0.007	0.47

Mechanism for the oxide formation

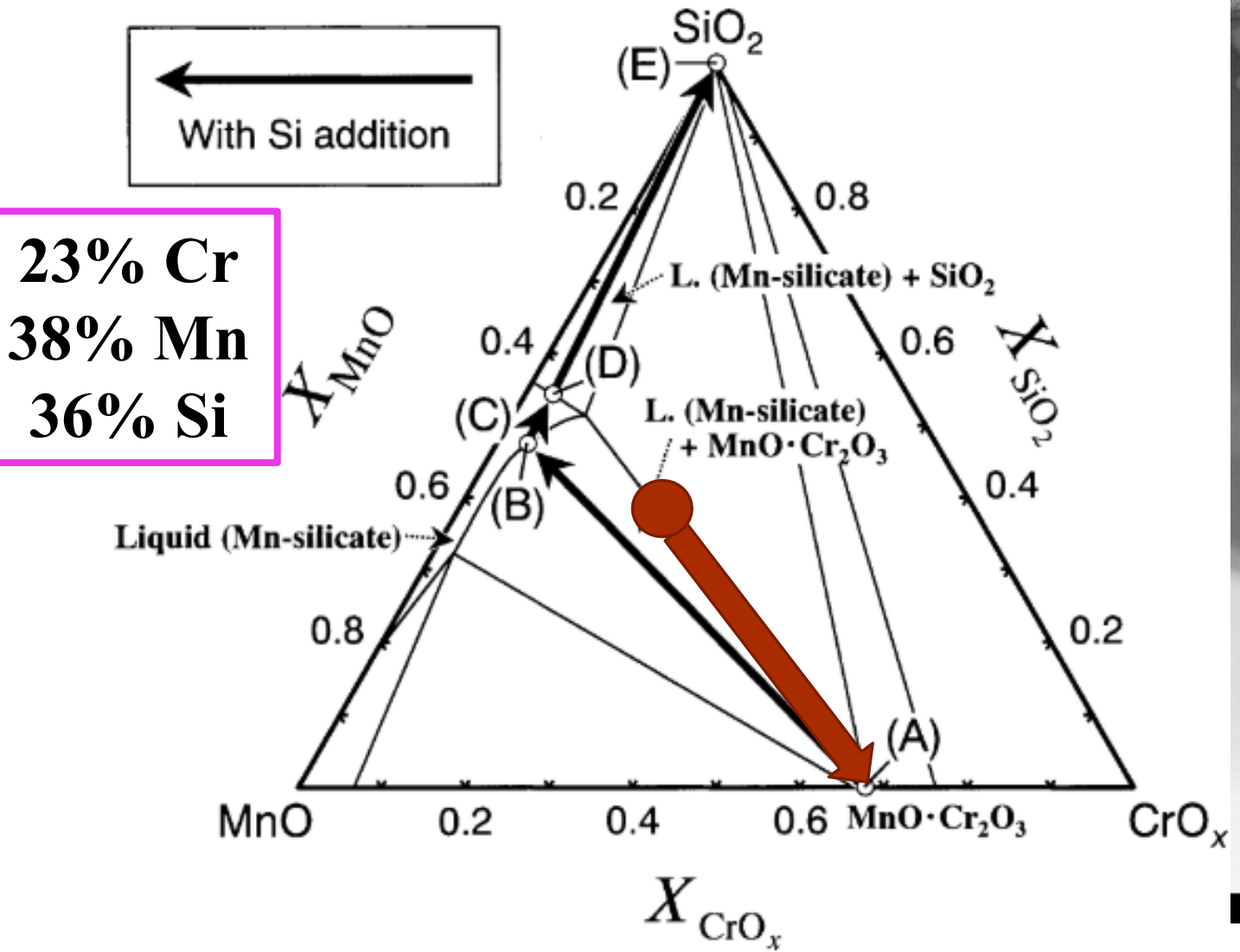
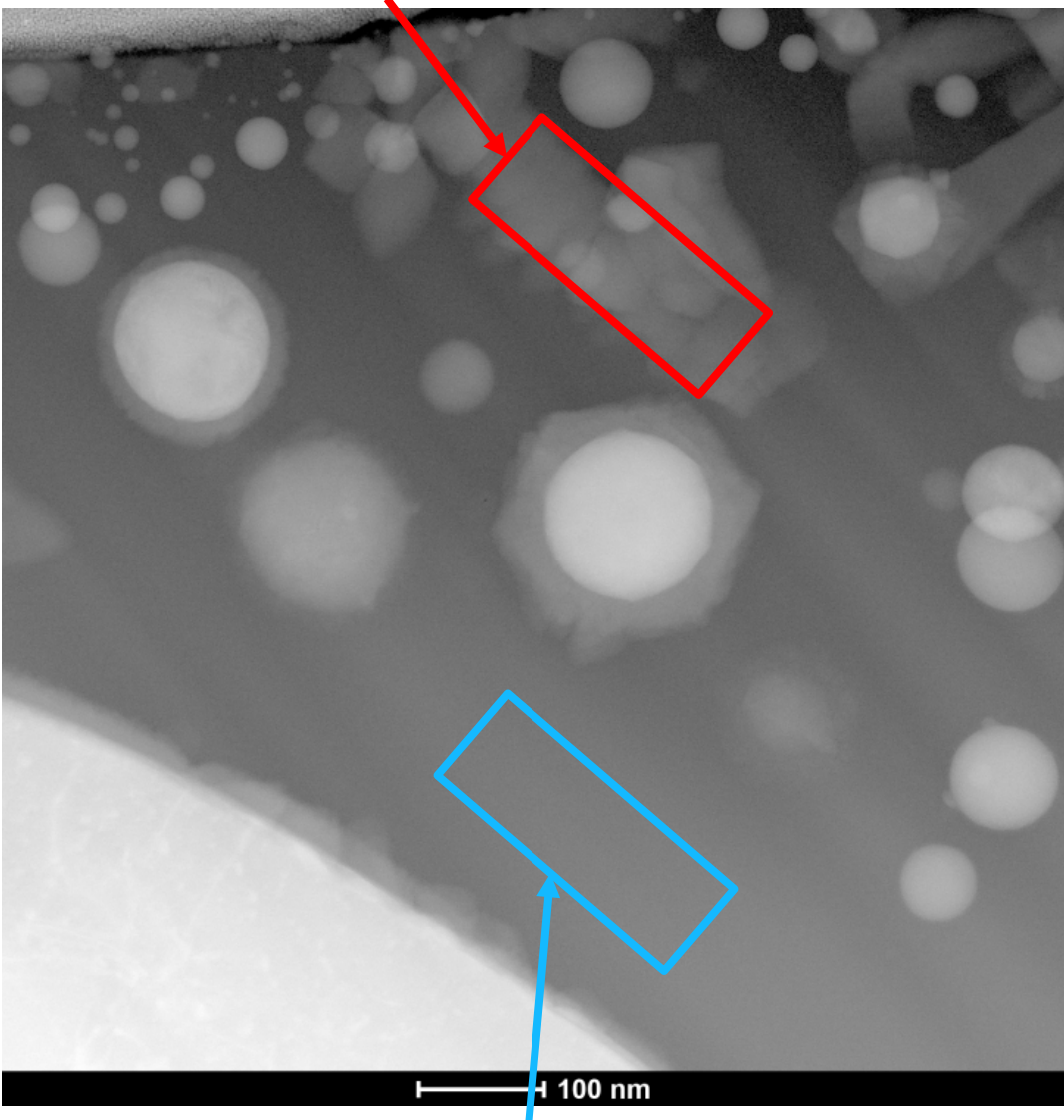


How and why do these oxides form?

36



70% Cr-30% Mn oxide



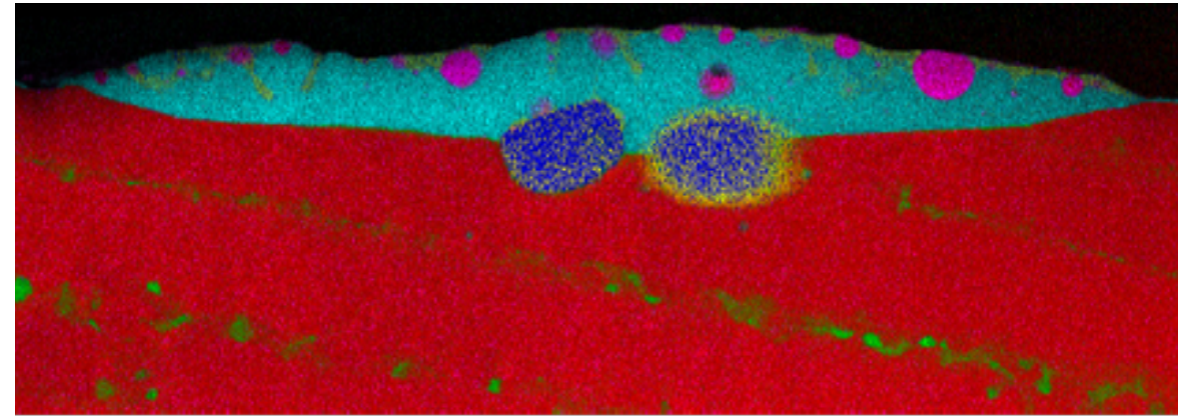
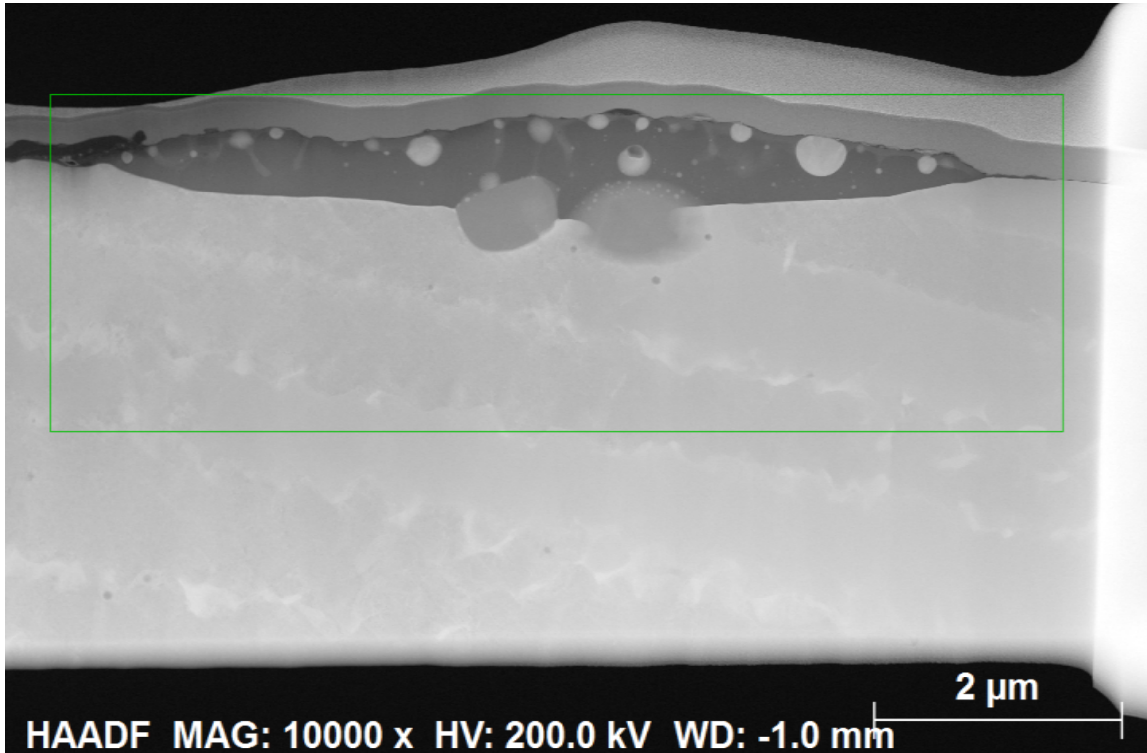
M. Tanahashi, et al., Phase Equilibria of the MnO, SiO₂, CrO_x System at 1873 K under Controlled Oxygen Partial Pressure, ISIJ Int., (2001).

(UUR)

23% Cr-38% Mn-36% Si-3% Al

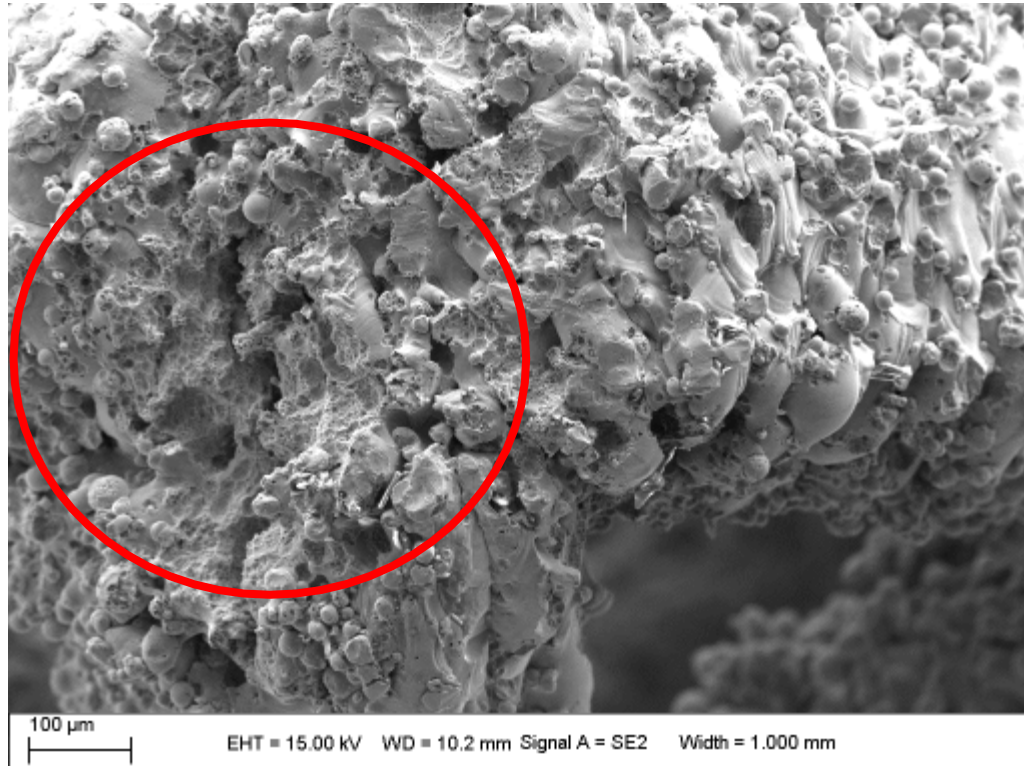
Oxides on Inconel 718 surface from SLM280

37

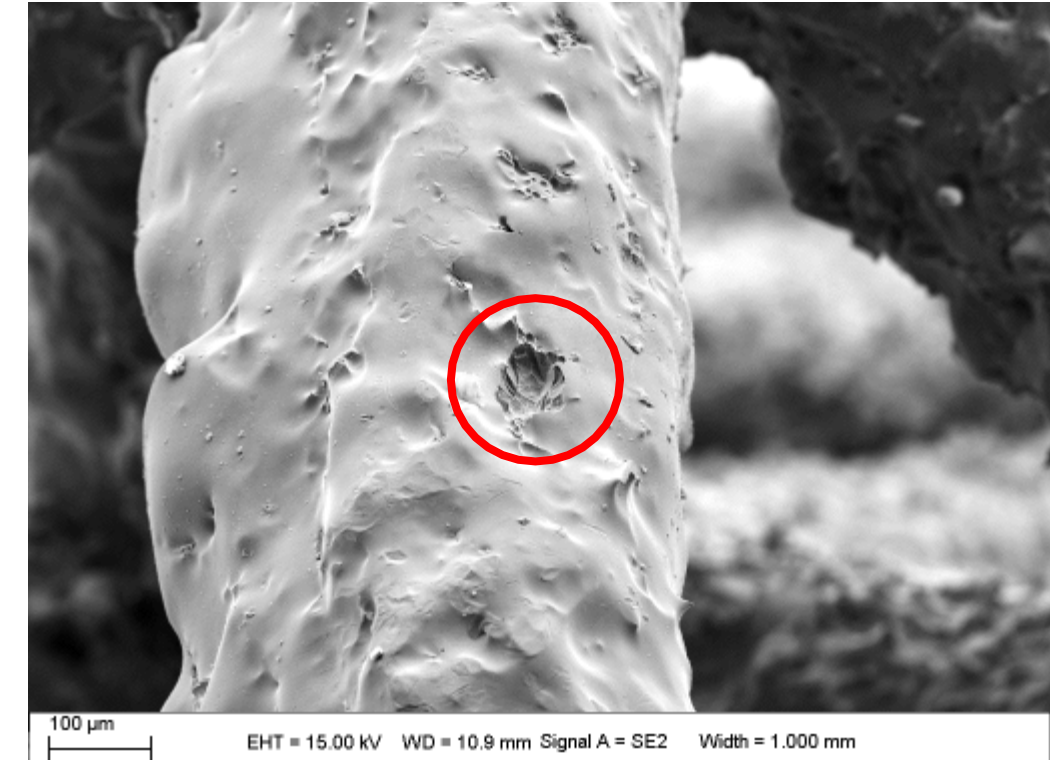


Pit morphology - Lattices

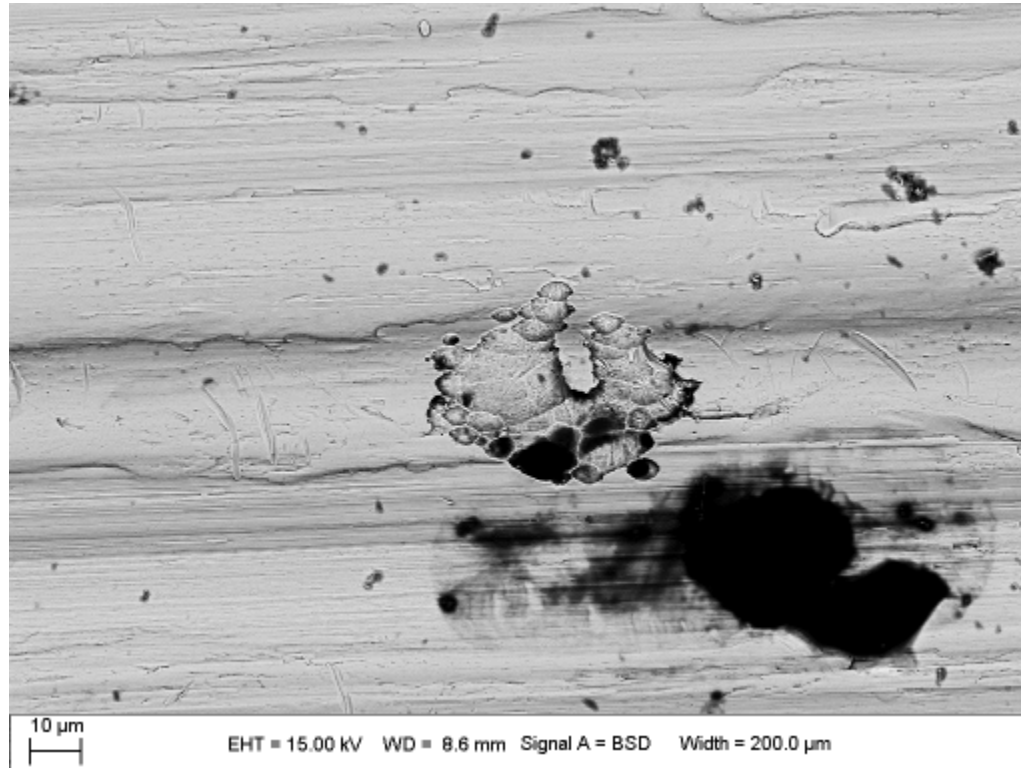
ProX 200
As-printed



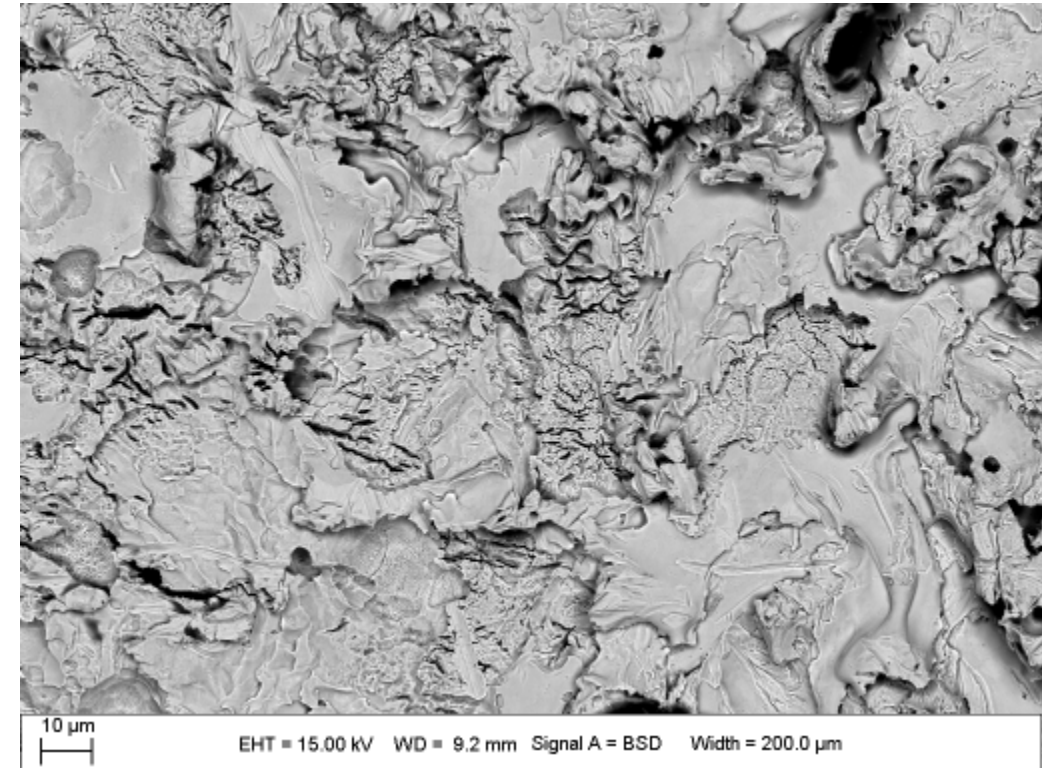
ProX 200
Electropolish



Bandsaw cut surface

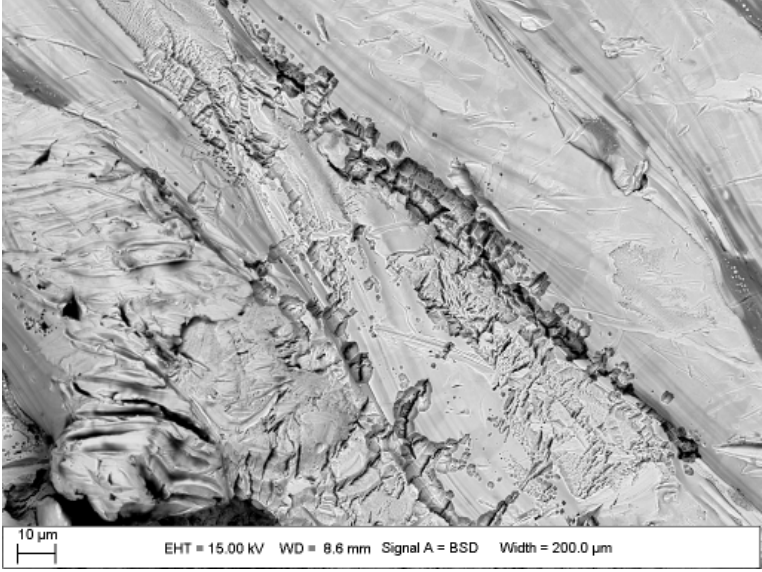


Wire EDM cut surface

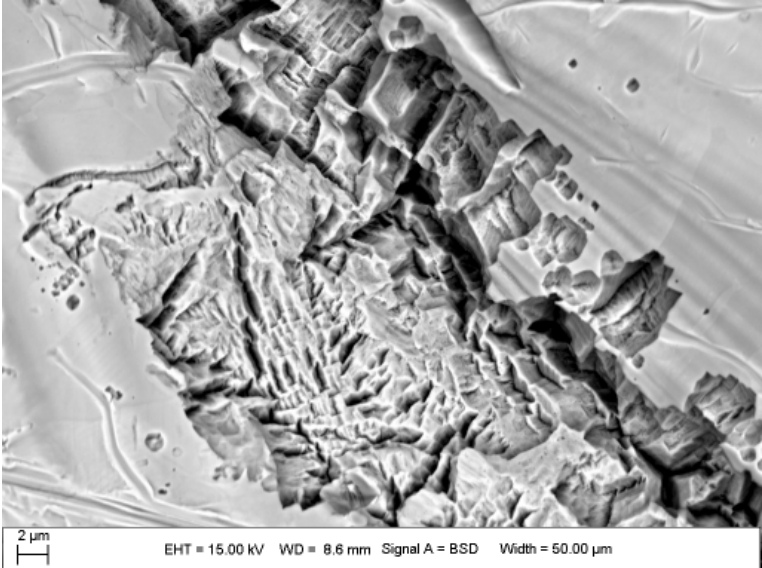


Pit morphology

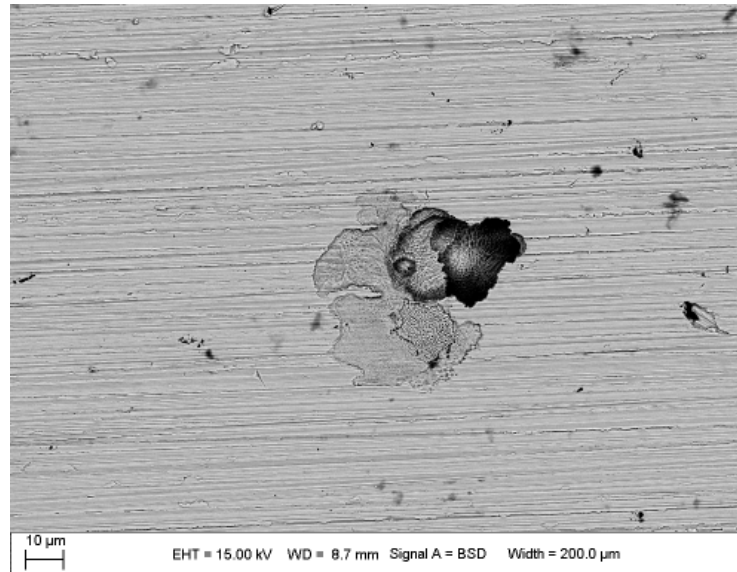
ProX 200 As-printed



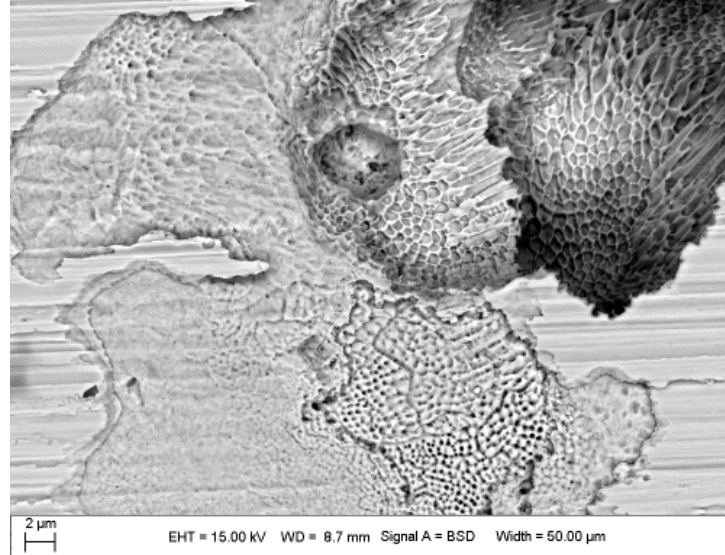
ASTM G85-A2



PBF316L (Renishaw)
surface was polished



40% RH - 300 µg/cm² of artificial sea water

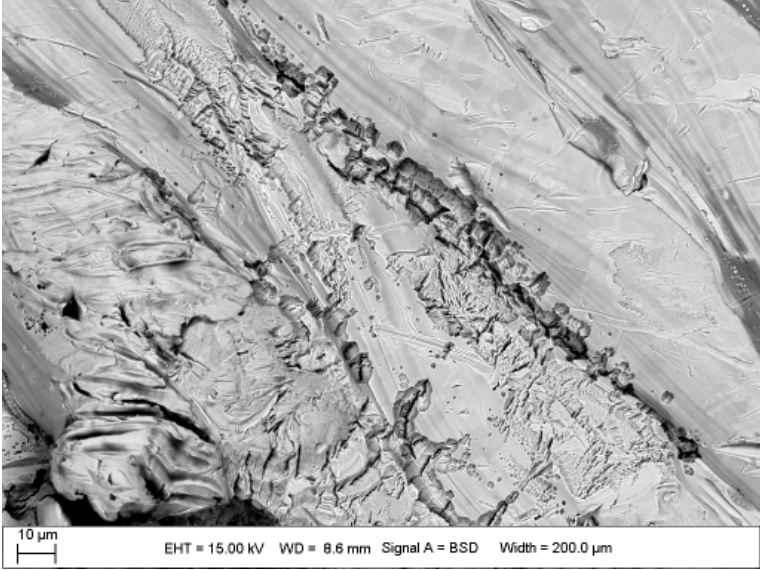


(UUR)



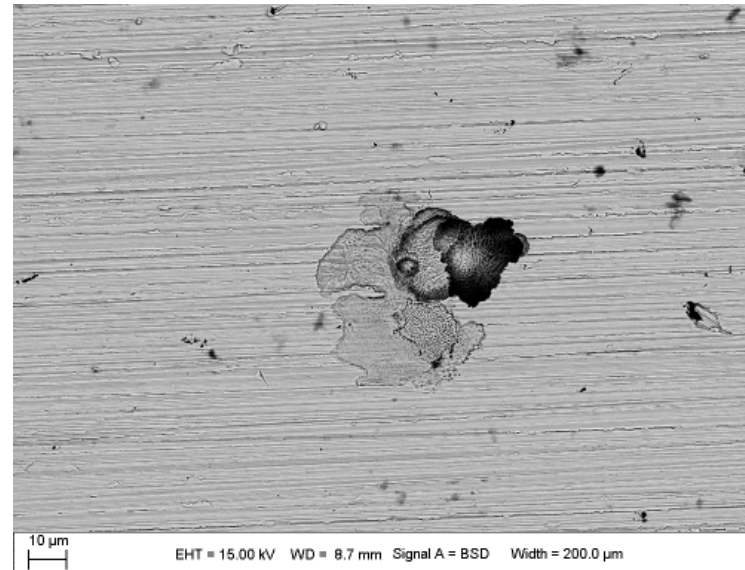
Pit morphology

ProX 200 As-printed

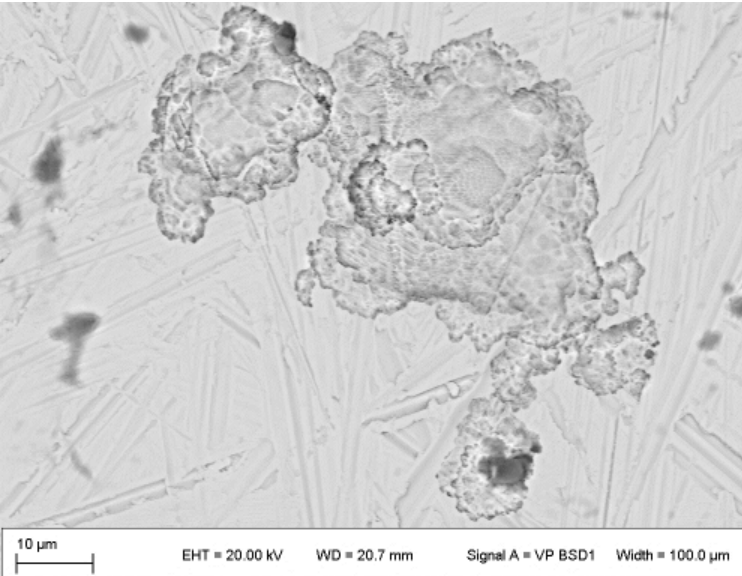


ASTM G85-A2

PBF316L (Renishaw)
surface was polished



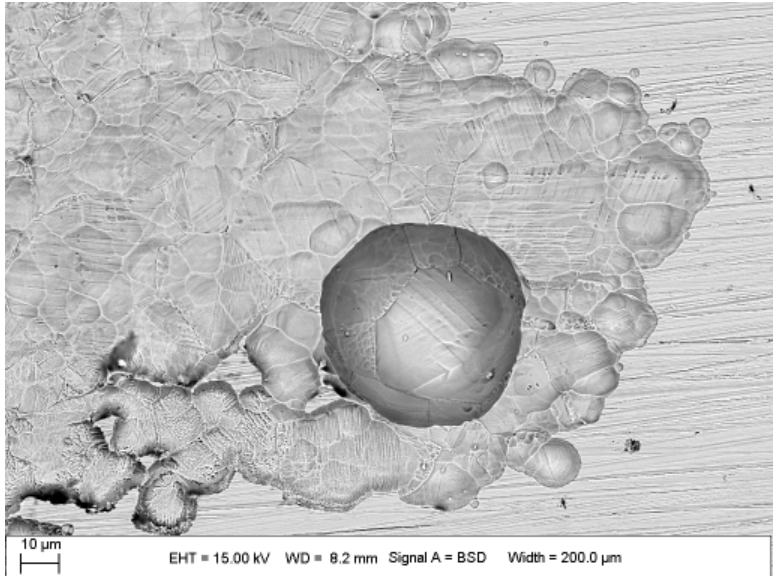
40% RH - 300 µg/cm² of artificial sea water



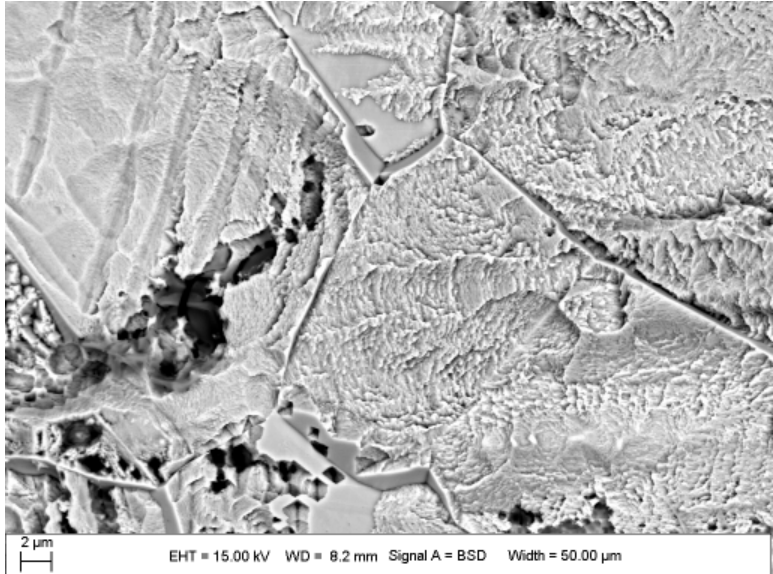
*From 21 month
exposure off coast of
Florida*

Pit morphology

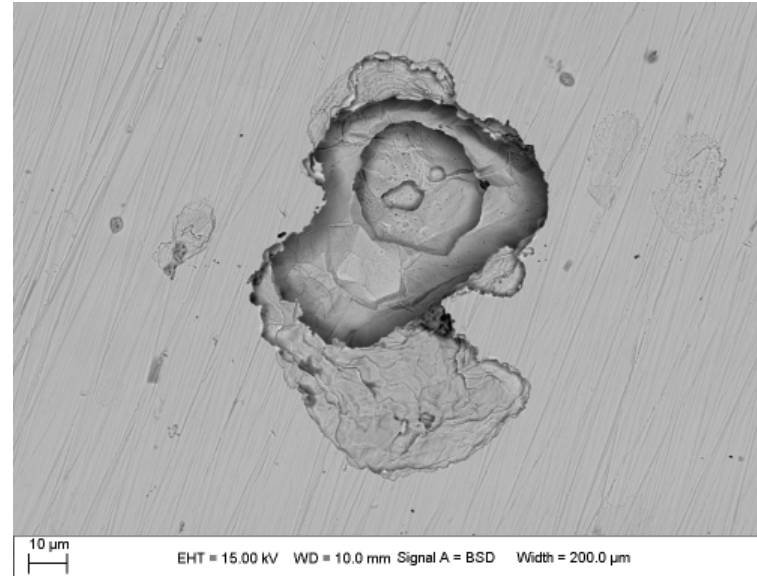
Wrought surface was polished



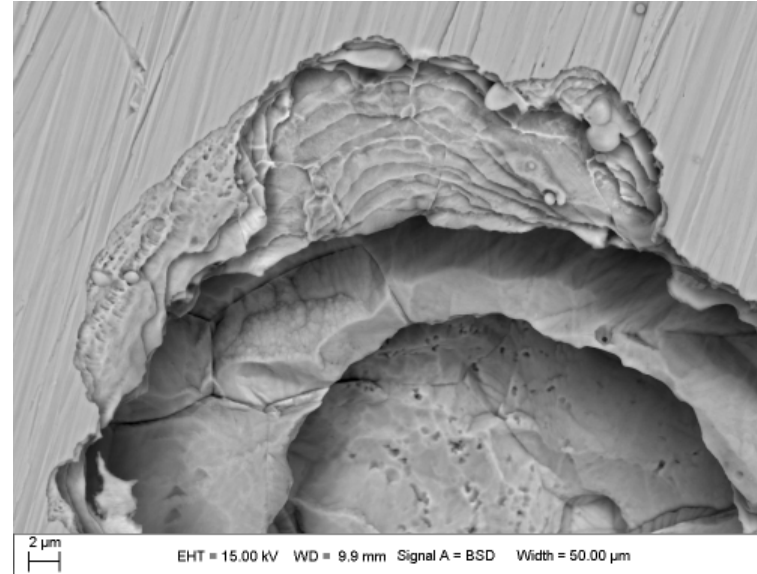
ASTM G85-A2



Wrought surface was polished



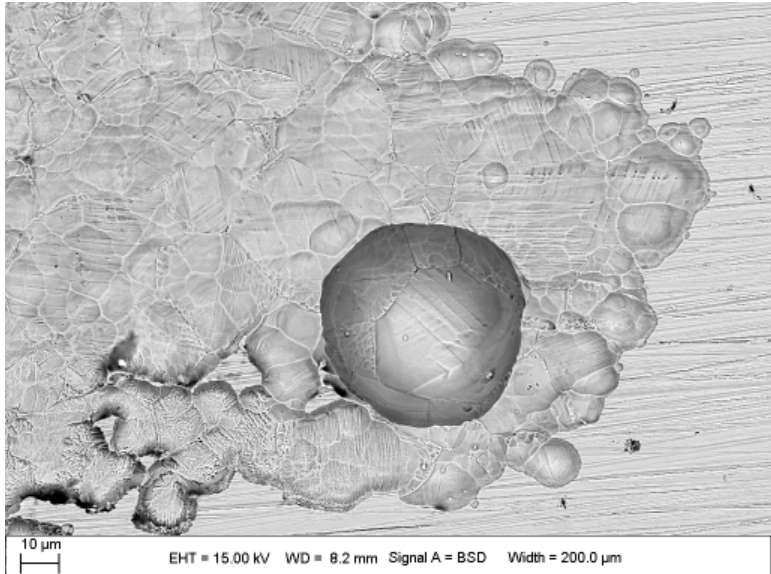
40% RH - 300 µg/cm² of artificial sea water



(UUR)

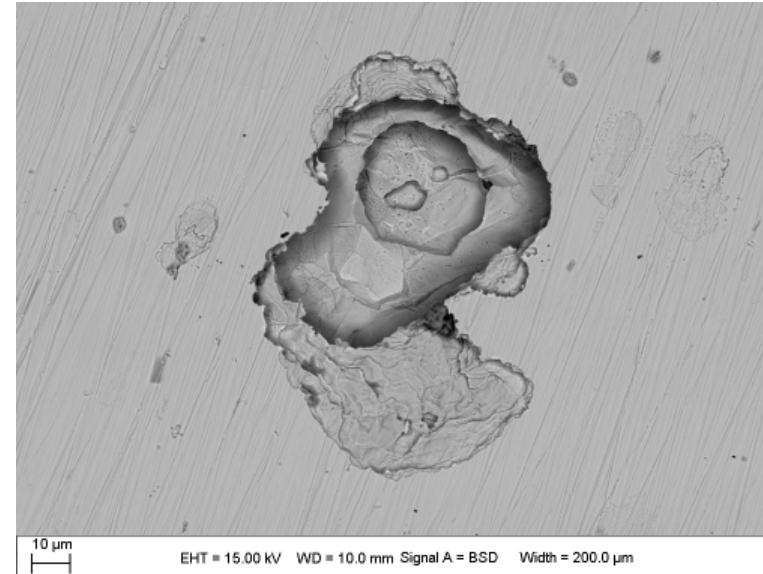
Pit morphology

Wrought surface was polished

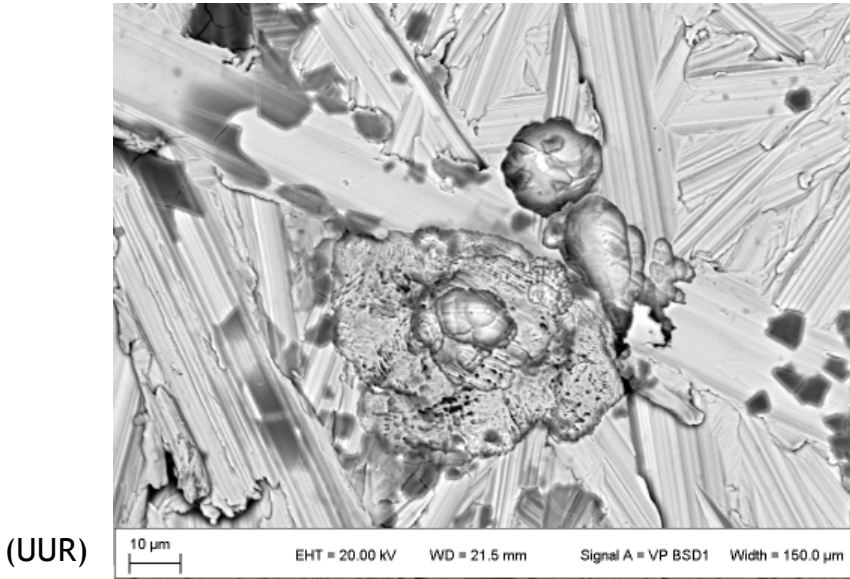


ASTM G85-A2

Wrought surface was polished



40% RH - 300 μg/cm² of artificial sea water

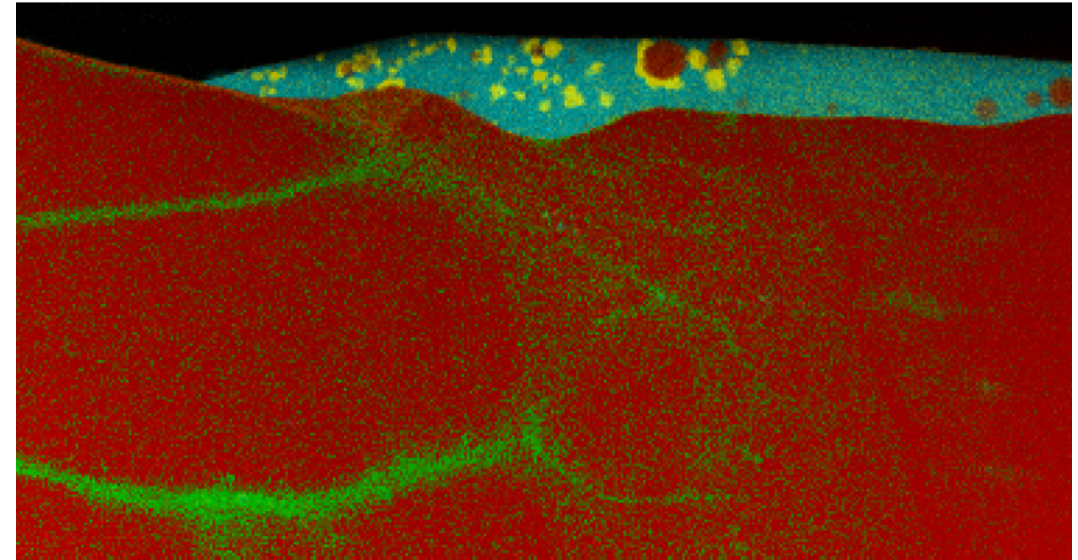
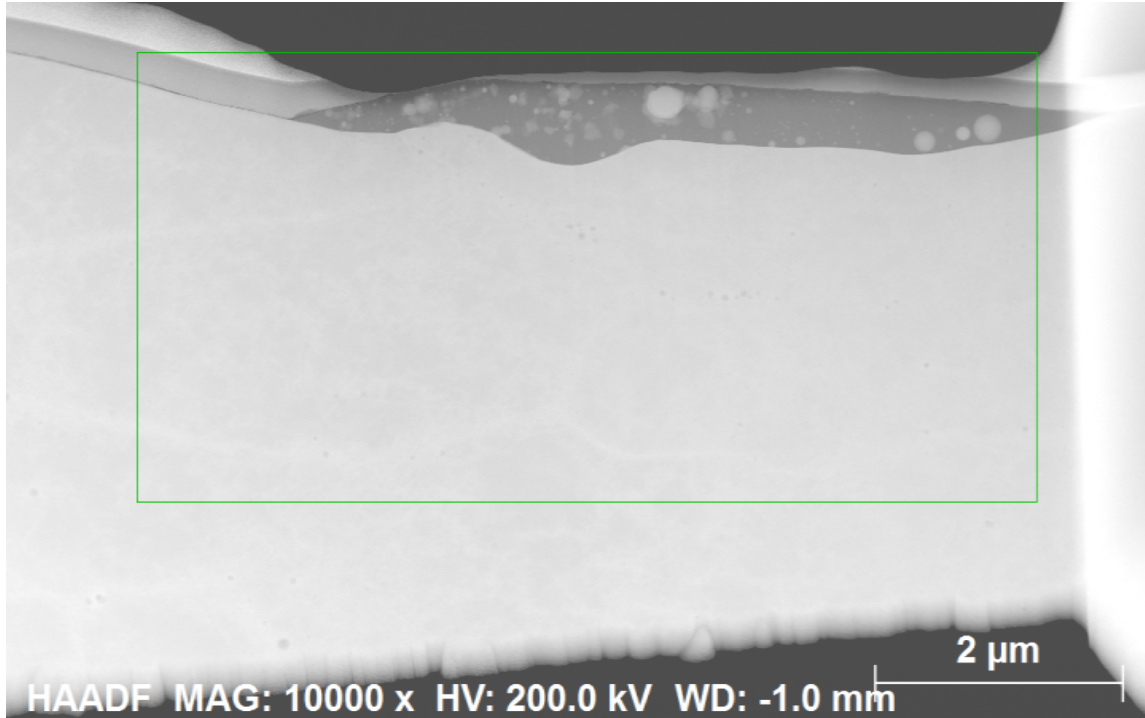


(UUR)

*From 21 month
exposure off coast of
Florida*

Oxides on 316L surface from EOS290

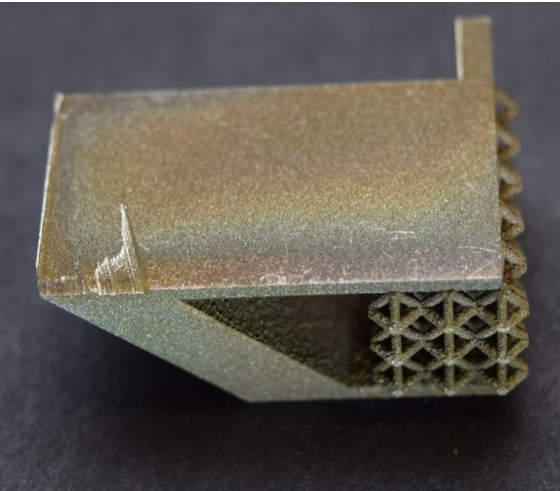
44



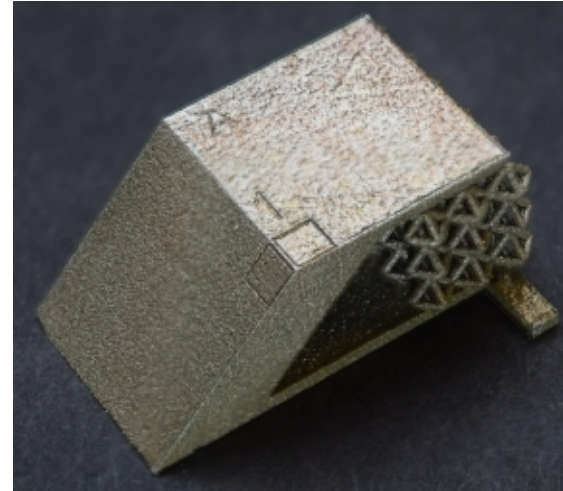
Wire EDM recast layer from ProX200



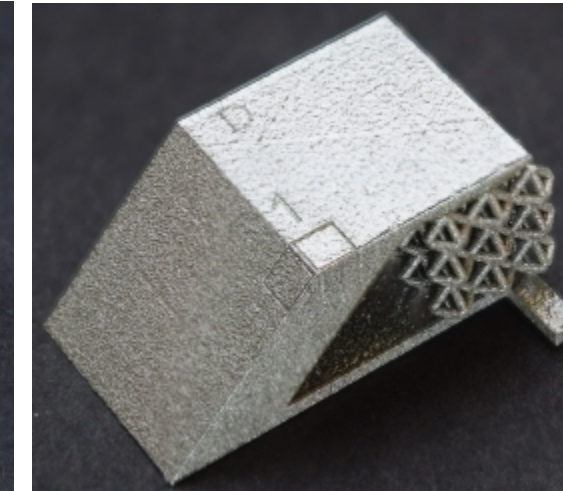
Wire EDM cut surface



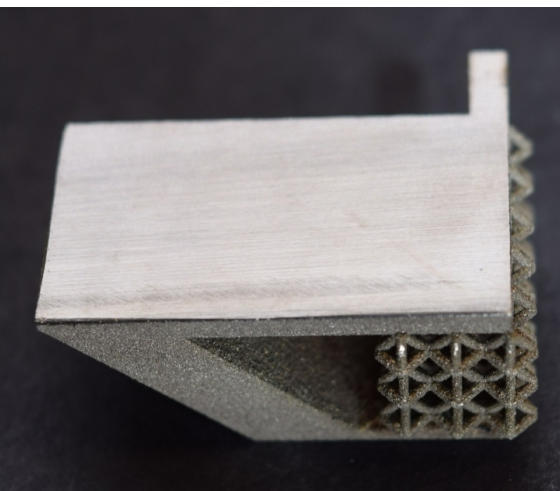
Wire EDM Top view



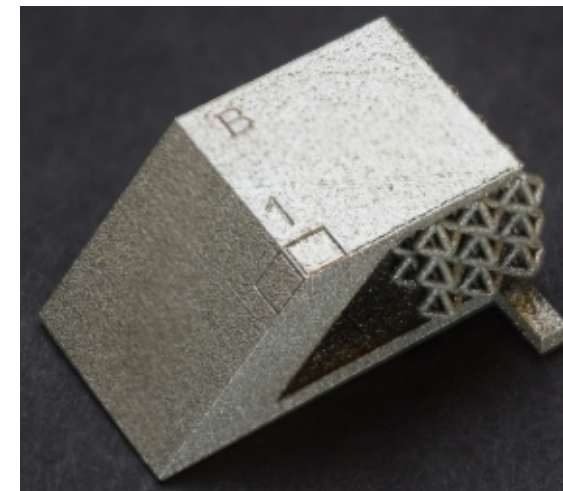
Rustripper Top view



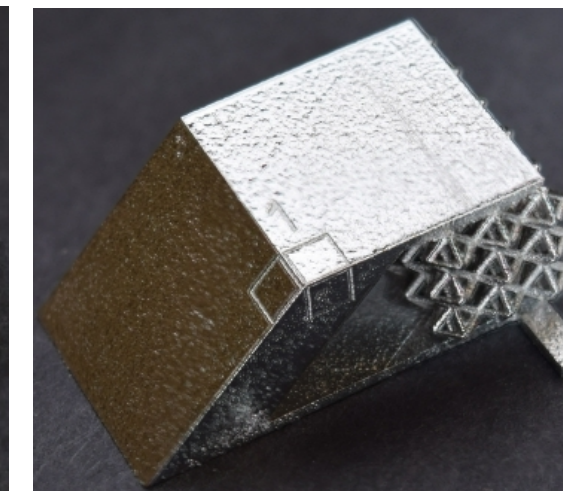
Bandsaw cut surface



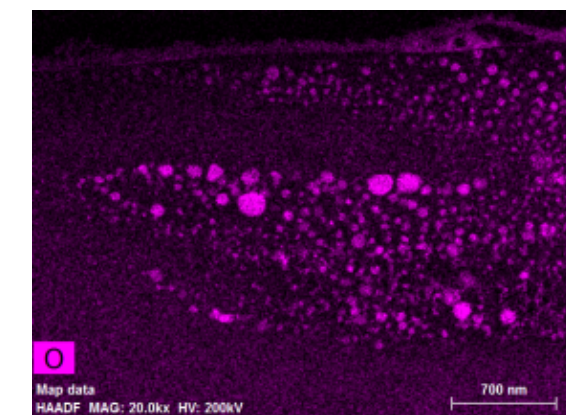
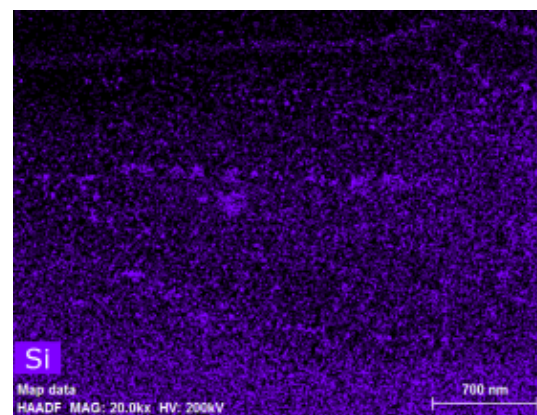
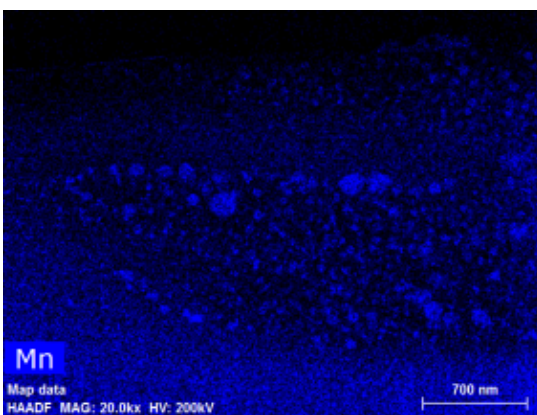
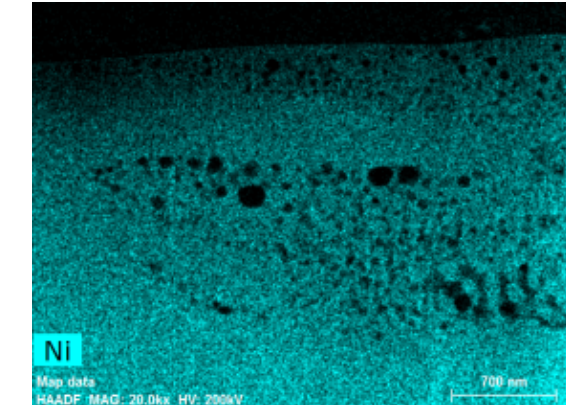
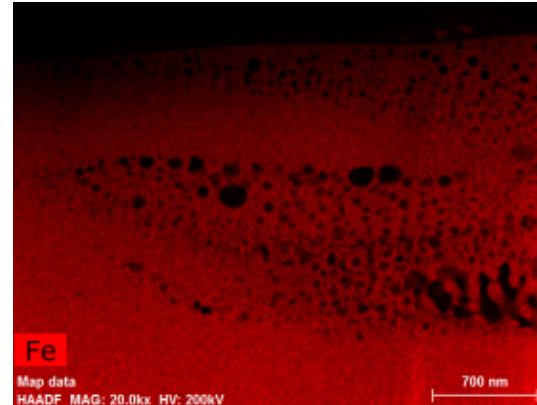
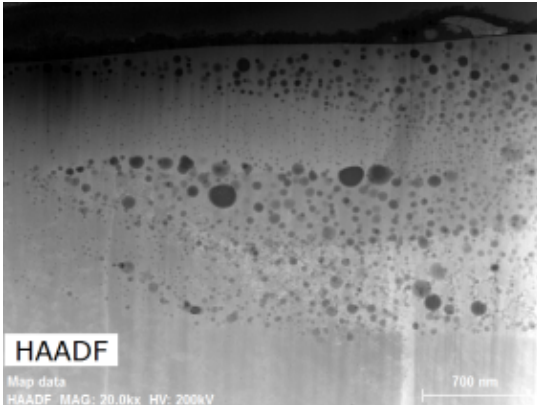
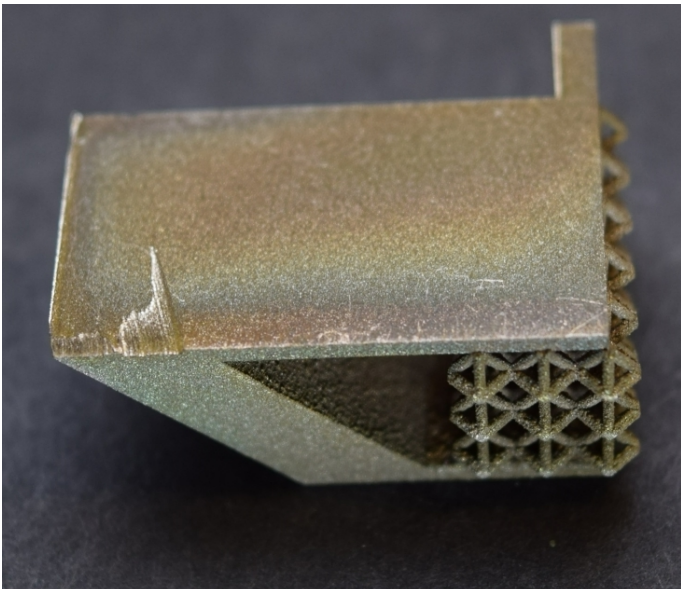
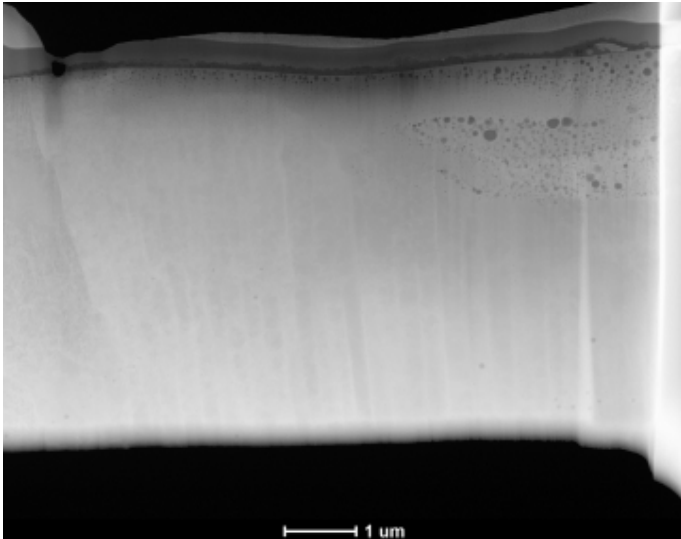
Bandsaw Top view



Electropolished Top view

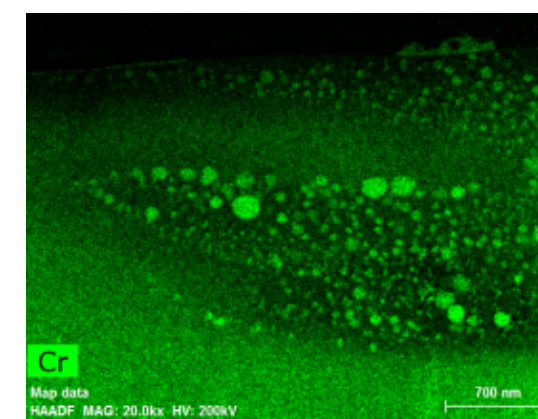
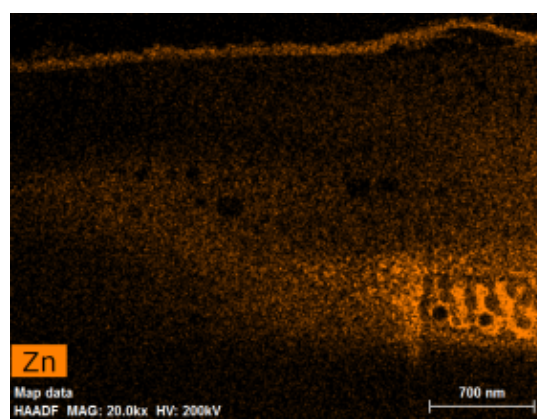


STEM/EDS of *wire EDM recast layer* from ProX200



Assuming Cu
is in similar
area as Zn

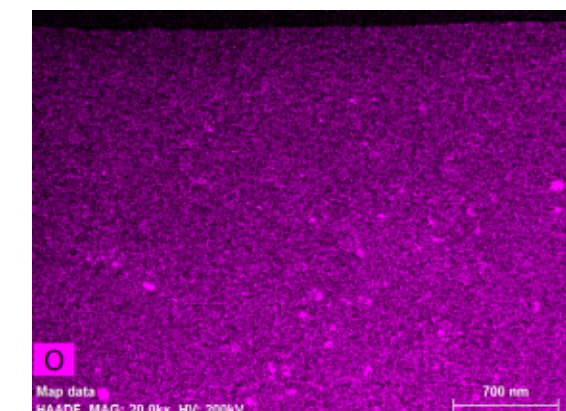
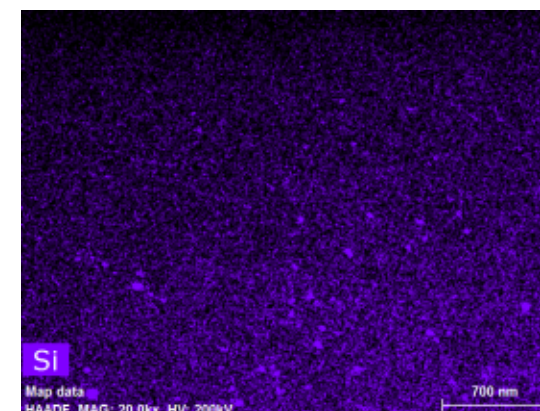
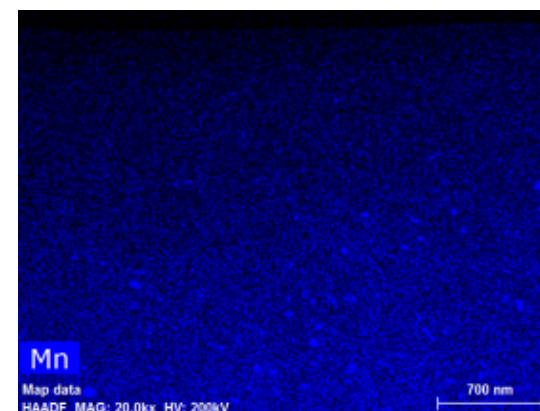
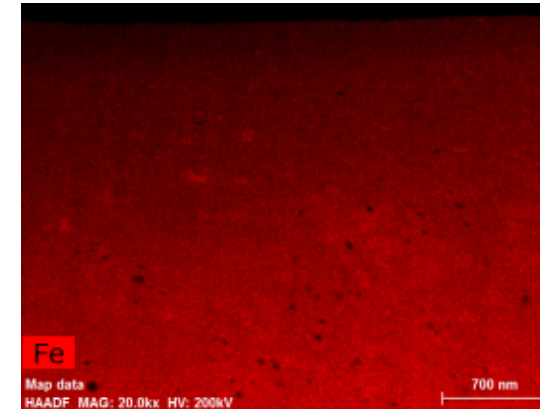
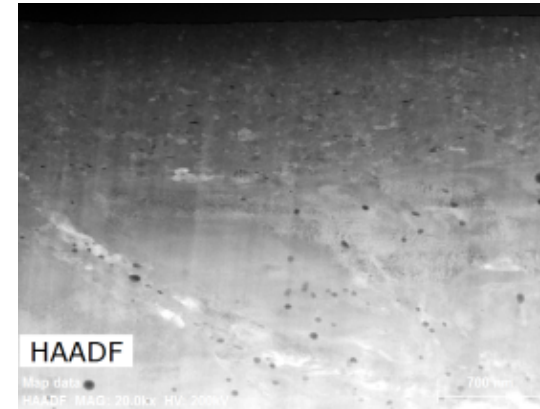
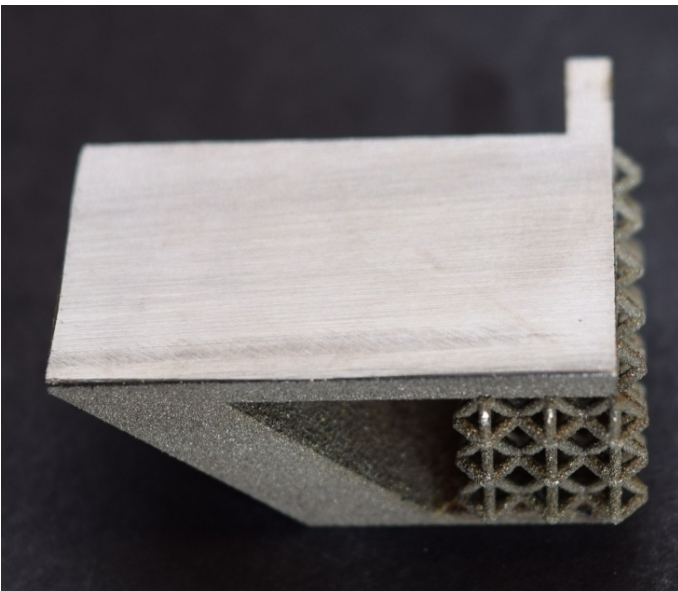
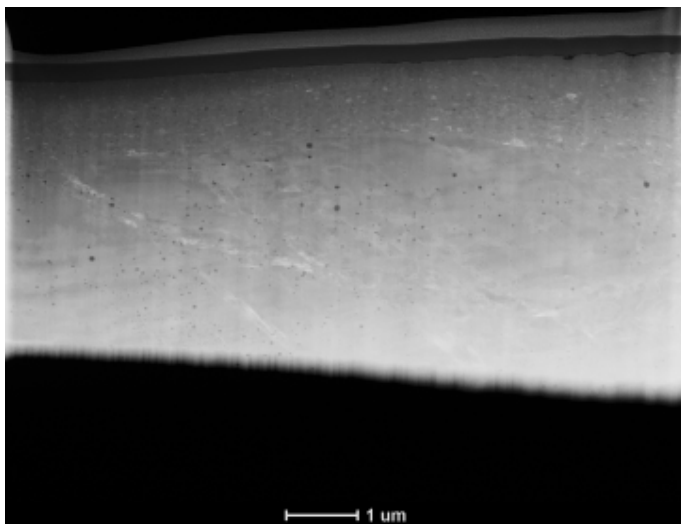
(UUR)



~2 μm thick

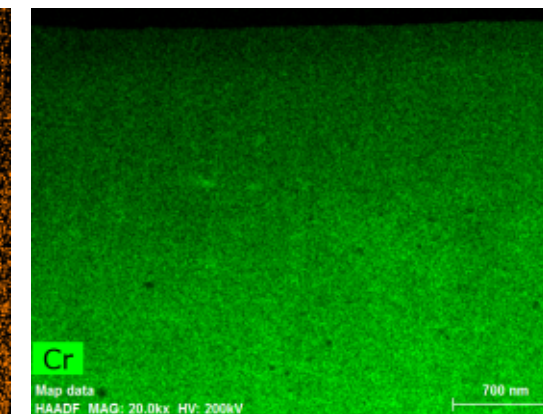
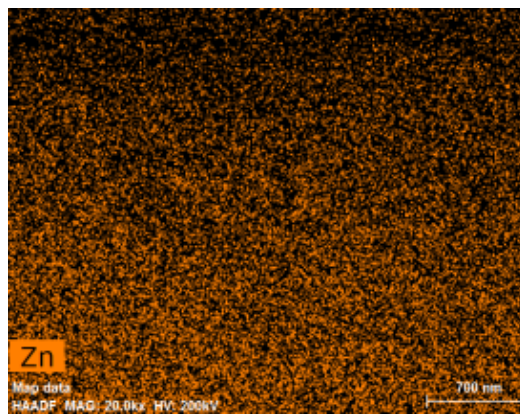
Courtesy:
Paul Kotula

STEM/EDS of *Bandsaw deformed layer* from ProX200



Assuming Cu
is in similar
area as Zn

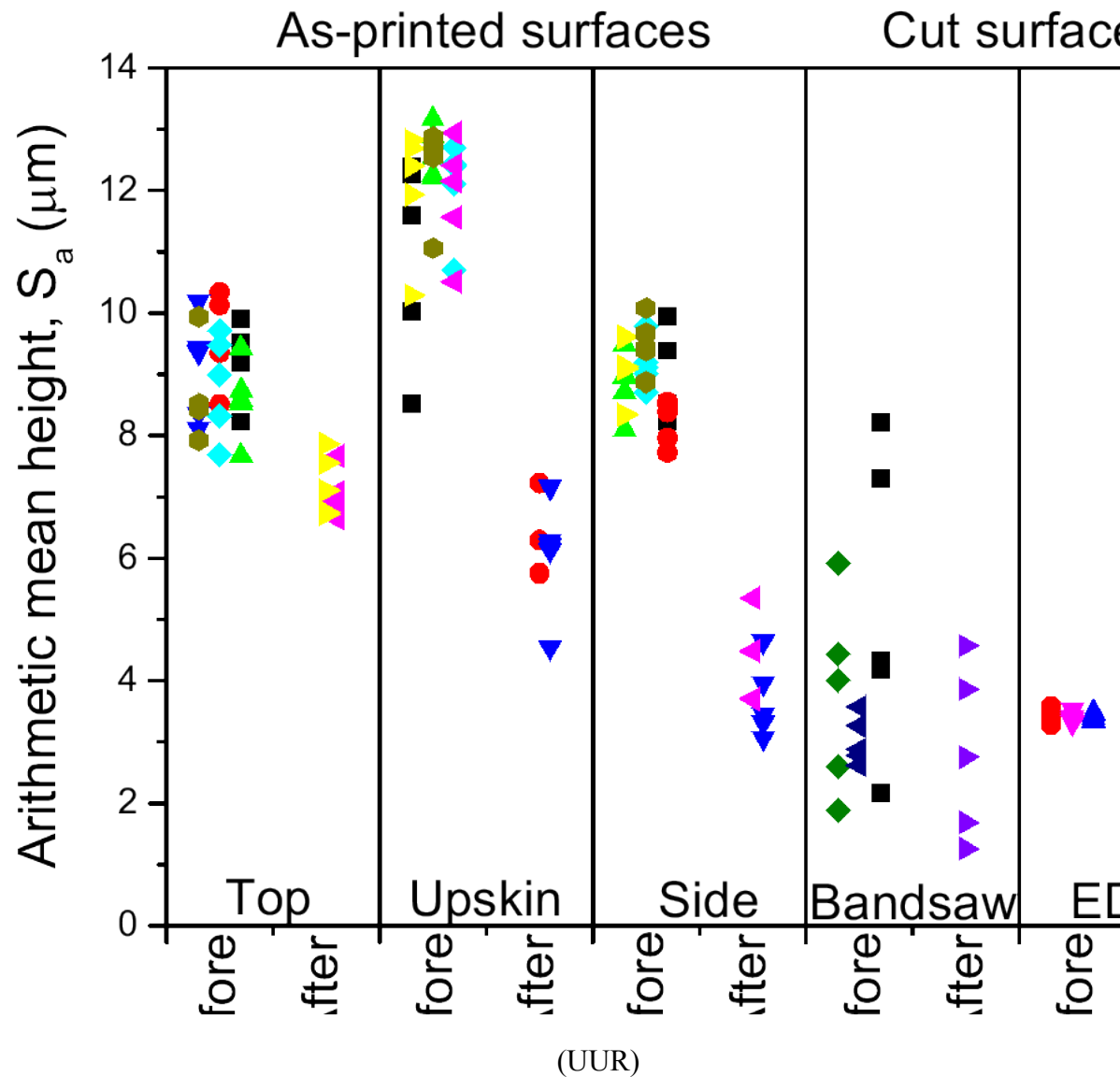
(UUR)

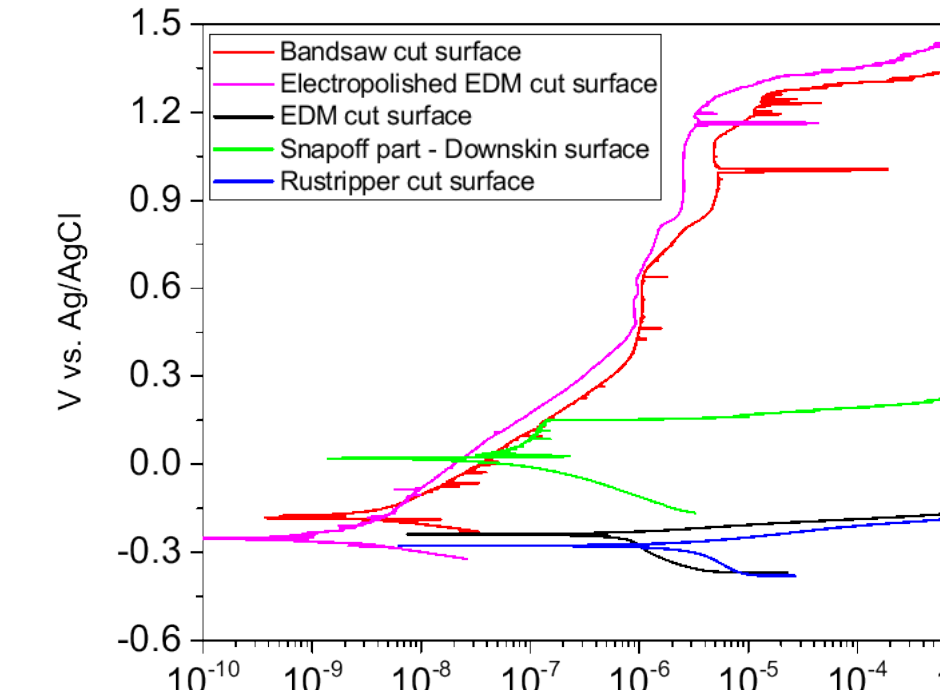
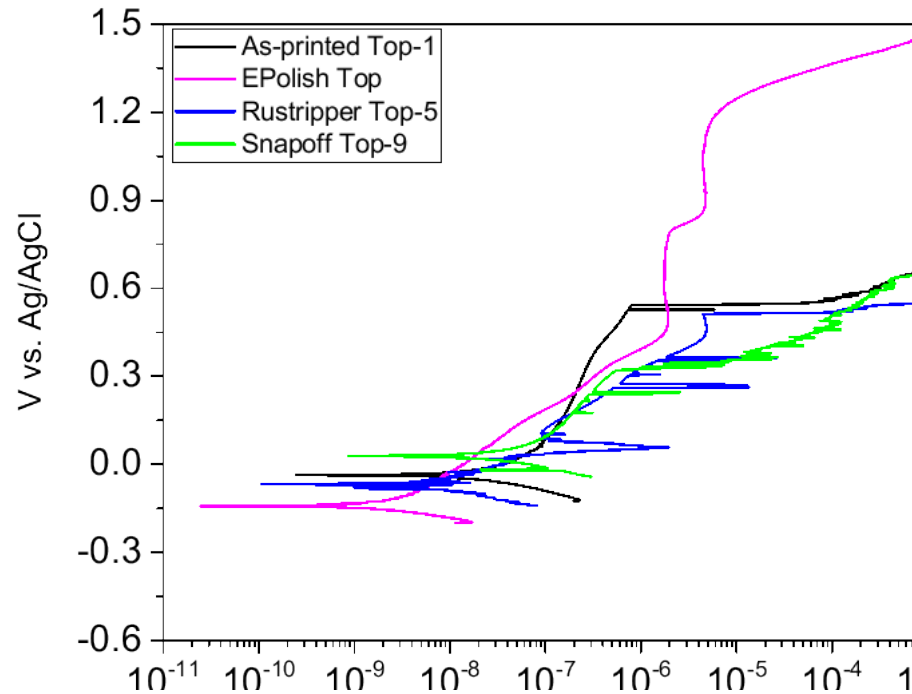


~1.4 μm
thick

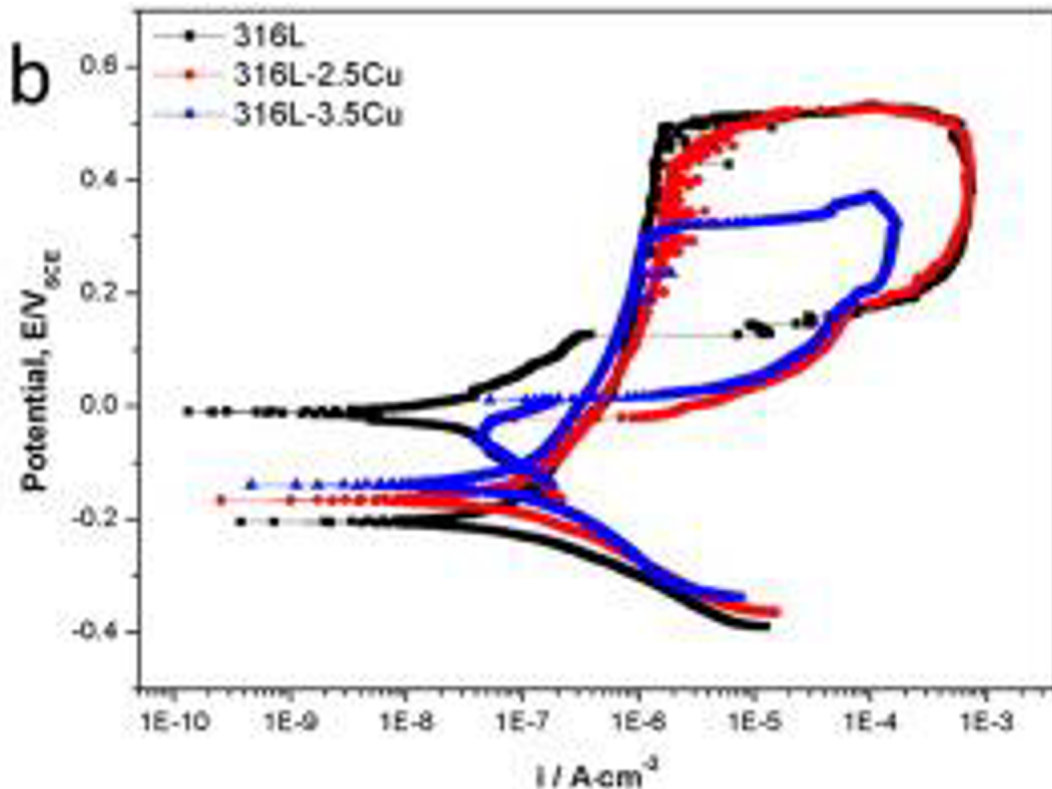
Courtesy:
Paul Kotula

Surface Roughness for ProX200 Before/After Electropolish

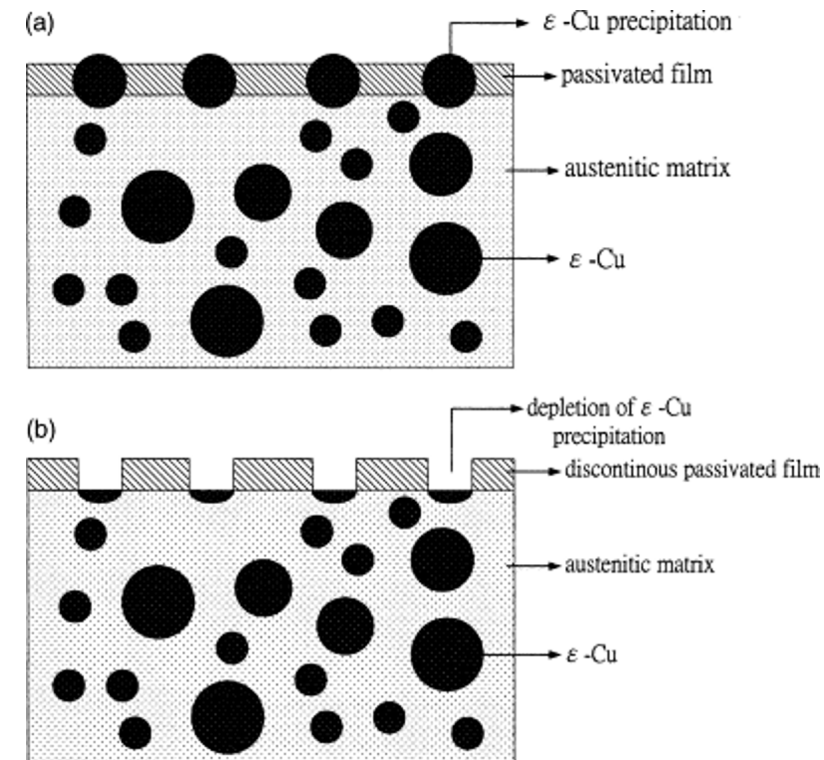




Cu additions to steel and corrosion response



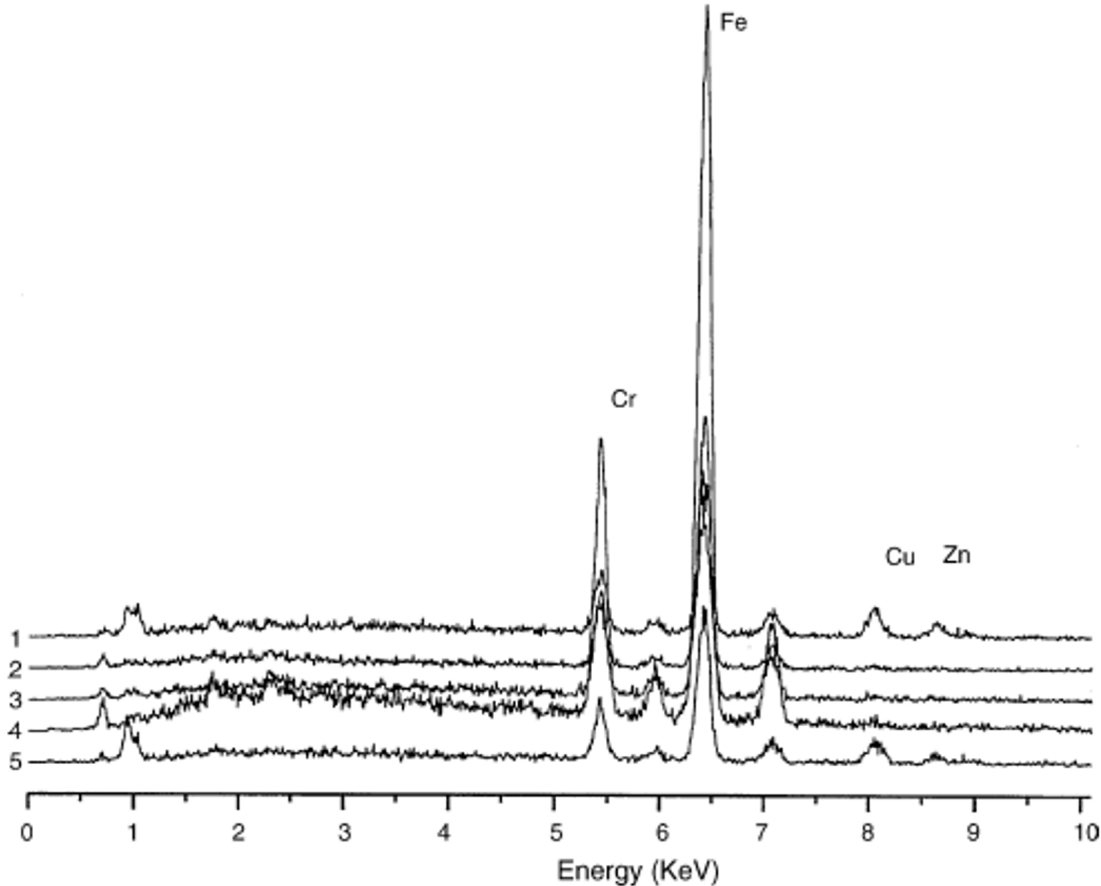
T. Xi, *Materials Science and Engineering: C*, (2017)



I.T. Hong, *Materials Science and Engineering: A*, (2005).

Precipitation of epsilon phase can cause discontinuous passivated film.
Also exhibit galvanic coupling with stainless steel –can be anode or cathode so a hard to predict corrosion response.

Wire EDM with varying parameters – impact on corrosion



Cu and Zn was abundant in cut 1 and 5, which correlate to the highest passive current density.

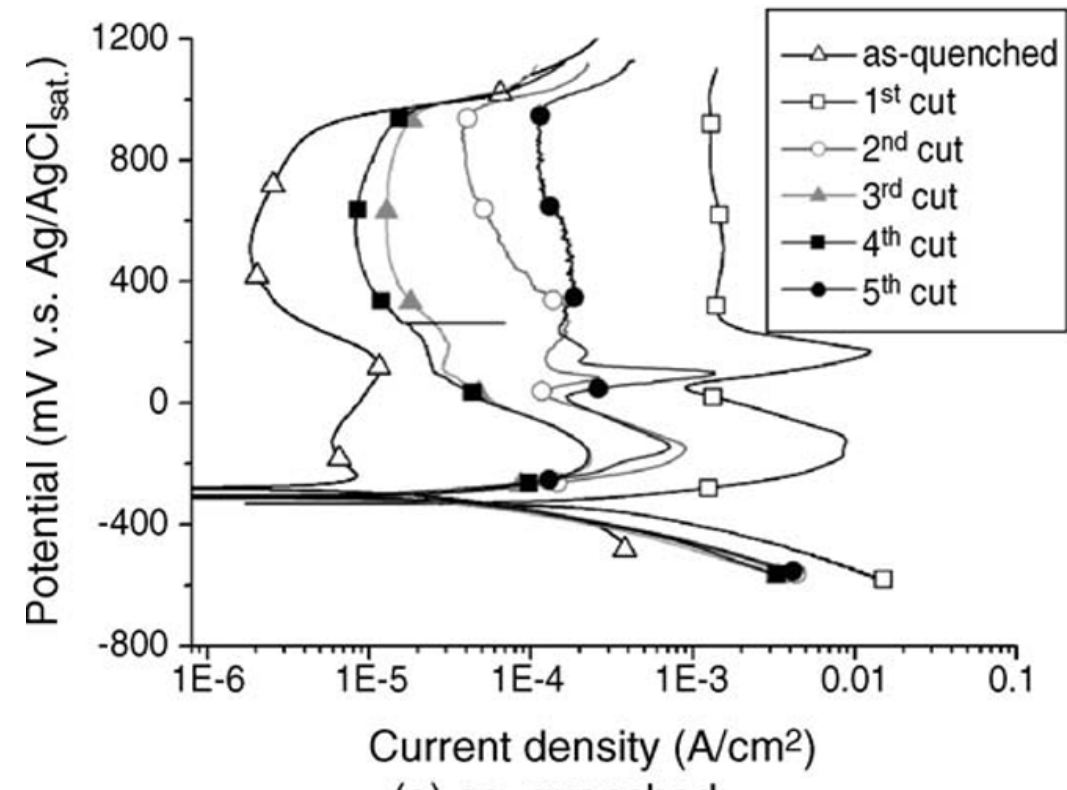
All cut surfaces showed an increase in passive current density (correlating to lower corrosion resistance).

Machining parameters used for multi-cutting passes with WEDM

Cutting pass	Voltage (V)	CD (A)	TA (μs)	TB (μs)	WS (m/min)	WB (daN)	FP (bar)
1st-cut	-80	4	1.0	9.0	10	1.0	5.5
2nd-cut	-120	8	0.2	3.8	8.0	1.4	0.8
3rd-cut	-80	16	0.4	3.0	8.0	1.4	0.8
4th-cut	-80	8	0.4	3.6	8.0	1.6	0.8
5th-cut	+120	4	0.2	3.8	8.0	1.4	0.8

CD: discharging current; TA: duration of discharging time; TB: time between two pulses; WS: wire feeding speed; WB: wire tension; FP: flushing pressure.

0.5 M HClO₄ and 0.2 M NaCl solution



C.A. Huang, Appl. Surf. Sci., (2006)